

Numerical Solution of System of N -Coupled Nonlinear Schrödinger Equations via Two Variants of the Meshless Local Petrov–Galerkin (MLPG) Method

M. Dehghan¹, M. Abbaszadeh² and A. Mohebbi³

Abstract: In this paper three numerical techniques are proposed for solving the system of N -coupled nonlinear Schrödinger (CNLS) equations. Firstly, we obtain a time discrete scheme by approximating the first-order time derivative via the forward finite difference formula, then for obtaining a full discretization scheme, we use the Kansa's approach to approximate the spatial derivatives via radial basis functions (RBFs) collocation methodology. We introduce the moving least squares (MLS) approximation and radial point interpolation method (RPIM) with their shape functions, separately. It should be noted that the shape functions of RPIM unlike the shape functions of the MLS approximation have kronecker delta property. Also, we implement the local meshless Petrov-Galerkin (MLPG) and local RPIM (LRPIM) techniques for obtaining two full discretization schemes for the numerical solution of the mentioned equation in the two-dimensional case. In the meshless local weak forms for obtaining an approximate solution for the node i in every sub-domain we use the shape functions of the moving least squares (MLS) and RPIM meshless approximations. The main aim of this paper is to show that the meshless methods based on the global form i.e. radial basis functions collocation method and local weak form i.e. MLPG and LRPIM techniques are also simple in implementation and suitable for the treatment of the system of coupled nonlinear Schrödinger equations. We show that the RBFs collocation scheme provides a simple implementation for computing long-range solitary solutions considered by coupled nonlinear Schrödinger equations and the conserved quantities mass and energy almost are constant. Of course selecting small enough time step, obtains

¹ Department of Applied Mathematics, Faculty of Mathematics and Computer Science, Amirkabir University of Technology, No. 424, Hafez Ave., 15914, Tehran, Iran, Corresponding author. Emile: mdehghan@aut.ac.ir , mdehghan.aut@gmail.com, (M. Dehghan)

² Department of Applied Mathematics, Faculty of Mathematics and Computer Science, Amirkabir University of Technology, No. 424, Hafez Ave., 15914, Tehran, Iran. Email: m.abbaszadeh@aut.ac.ir (M. Abbaszadeh)

³ Department of Applied Mathematics, Faculty of Mathematical Science, University of Kashan, Kashan, Iran. Email: a_mohebbi@kashanu.ac.ir (A. Mohebbi), .

conserved quantities which are exactly fixed. Also several test problems including the two-dimensional case are given and numerical simulations are reported. We compare the obtained numerical results with together. The numerical results confirm the efficiency of the proposed schemes.

Keywords: Nonlinear system of coupled nonlinear Schrödinger equations(CNLS), Kansa's approach, meshless local Petrov-Galerkin technique(MLPG), moving least squares (MLS) approximation, radial point interpolation method (RPIM), radial basis functions(RBFs), forward finite difference scheme.

1 Introduction

Nonlinear phenomena play important roles in applied mathematics, physics and also in engineering [Ganji, Ganji, and Bararnia (2009)]. As said in [Noor, Noor, Waheeda, and Al-Said (2011)], many phenomena in engineering and applied sciences are modeled by nonlinear evolution equations. Solitary solutions [Helal (2002); Wazwaz (2009)] of nonlinear evolution equations provide better understanding of the physical mechanism of phenomena. The knowledge of closed form solutions of the nonlinear partial differential equations facilitates the testing of numerical solvers, aids in the stability analysis of solutions and leads to a better understanding of nonlinear phenomena that have been modeled by these equations [Gomez, Salas, and Frias (2010)]. Also, the search of exact solution for the nonlinear partial differential equations is very difficult. Therefore, numerical methods are useful for solving nonlinear partial differential equations. Recently, various analytical and semi-analytical methods for solving the nonlinear evolution equations have been developed and are applied for solving several partial differential equations (PDEs) and ordinary differential equations (ODEs) such as the inverse scattering method [Ablowitz and Clarkson (1991)], the Darboux transform [Matveev and Salle (1991)], the Hirota bilinear method [Hirota and Satsuma (1981)], the Painlevé expansion method [Weiss, Tabor, and Carnevale (1983)], the Bäcklund transformation method [Miura (1978)], the tanh-function method [Fan (2000)], the homogeneous balance method [Wang, Zhou, and Li (1996)], the Jacobi elliptic function expansion method [Liu, Fu, Liu, and Zhao (2001)], the F-expansion method [Wang and Li (2005)], and etc. Also we refer the interested reader to [Wazwaz (2008);Wazwaz (2006)] for some other approaches.

1.1 Application of the Schrödinger models

In this paper, we consider the (CNLS) equations to the following form

$$i \frac{\partial \Psi_n}{\partial t} + \alpha_n \frac{\partial^2 \Psi_n}{\partial x^2} + \left(\sum_{m=1}^n \sigma_{nm} |\Psi_m|^2 \right) \Psi_n = 0, \quad -\infty < x < \infty, \quad n = 1, 2, \dots, N, \quad (1)$$

where Ψ_n , $n = 1, 2, \dots, N$ are complex valued wave amplitudes, i is an imaginary number and also x and t represent space and time variables, respectively. The parameters α_n , $n = 1, 2, \dots, N$ are group velocity dispersion (GVD) coefficients, σ_{nn} , $n = 1, 2, \dots, N$ are self-phase modulation (SPM) coefficients, which are also known as the Landau constants, and σ_{nm} , $n \neq N$ are cross phase modulations or wave-wave interaction coefficients.

Also, we present conservation laws, which are most prominent for testing performance of numerical schemes for CNLSE. In the current paper, we only select two conserved properties i.e. mass and energy.

- mass conservation [Bhatt and Khaliq (2014)]:

$$I_i = \int_{x_L}^{x_R} |\Psi_i|^2 dx \quad \text{is a constant}, \quad i = 1, 2, \dots, N, \quad (2)$$

- energy conservation [Bhatt and Khaliq (2014)]:

$$\|\Psi_j\|_2 = \sqrt{h \sum_{i=1}^M \Psi_j(x_i)}, \quad j = 1, 2, \dots, N. \quad (3)$$

The Schrödinger equation was proposed by physicist Erwin Schrödinger in 1926. It succeeded the quantum theory ideas of Planck which stated the quantization of energy and the great Einstein. It sparked the quantum mechanical era and disproved many concepts from classical mechanics¹. Schrödinger was the first person to write down such a wave equation. Much discussion then centered on what the equation meant. The eigenvalues of the wave equation were shown to be equal to the energy levels of the quantum mechanical system, and the best test of the equation happened when it was used to solve the energy levels of the Hydrogen atom, and

¹ <http://chemwiki.ucdavis.edu/Physical-Chemistry/Quantum-Mechanics/Quantum-Theory/Principle-of-Quantum-Mechanics/Schrödinger-Equation>

the energy levels were found to be in accord with Rydberg's Law. It was initially much less obvious what the wave function of the equation was. After much debate, the wave function is now accepted to be a probability distribution². As mentioned in³ the Schrödinger equation integrates both classical mechanics and optics. It uses conservation of energy from classical mechanics written in terms of its wave function. It is the basic equation used to solve wave functions of atomic particles such as electrons, protons, and atoms. The Schrödinger equation is used to find the allowed energy levels of quantum mechanical systems (such as atoms, or transistors). The associated wave function gives the probability of finding the particle at a certain position⁴. The nonlinear Schrödinger equation is widely used in basic models of nonlinear waves in many areas of physics and chemistry [Kavitha, Akila, Prabhu, Kuzmanovska-Barandovska, and Gopi (2011)]. As mentioned in [Kavitha, Akila, Prabhu, Kuzmanovska-Barandovska, and Gopi (2011)] the considered equation arises from the study of nonlinear wave propagation in dispersive and inhomogeneous media such as plasma phenomena and nonuniform dielectric media. As said in [Bhatt and Khaliq (2014)] the coupled nonlinear Schrödinger equations are highly used in modeling various phenomena in nonlinear fiber optics, like propagation of pulses. The system of coupled nonlinear Schrödinger equations (CNLSE) has been appeared in many areas in engineering and science for example in the area of hydrodynamics and fiber optics [Kivshar and Agrawal (2003); Mei (1989)]. As mentioned in [Bhatt and Khaliq (2014)] in nonlinear optics, the CNLSE models an optical soliton which is a special solitary wave that not only maintains its shape after wave interaction but travels long distance without any optical loss. This form of soliton is created by balancing the anomalous group velocity dispersion with the fiber nonlinearity, called self-phase modulation and offers unmodulated transfer of pulses from one place to another over a long distance. Also we refer the interested reader to [Dehghan and Shokri (2007); Dehghan and Mirzaei (2008); Helal and Seadawy (2009); Helal and Seadawy (2011)].

1.2 The literature review

Authors of [Ismail and Alamri (2004)] developed a numerical method for solving the CNLSE, which is fourth-order in space and second-order in time, unconditionally stable and studied the interaction of two solitons of different amplitudes. The finite difference schemes for solving a system of the nonlinear Schrödinger (NLS) equations were investigated in [Kurtinaitis and Ivanauska (2004)]. Also

² <http://answers.yahoo.com/question>

³ <http://chemwiki.ucdavis.edu/Physical-Chemistry/Quantum-Mechanics/Quantum-Theory/Principle-of-Quantum-Mechanics/Schrödinger-Equation>

⁴ <http://answers.yahoo.com/question>

several types of schemes, including explicit, implicit, Hopscotch-type and Crank-Nicolson-type are defined and cubic spline interpolation is used for solving time-shifting part of equations in the mentioned paper. Authors of [Sheng, Khaliq, and Al-Said (2001)] have concerned with a new conservative finite difference method for solving the generalized nonlinear Schrödinger (GNLS) equation and a numerical scheme is constructed through the semi-discretization approach and an application of the quartic spline approximation is presented. A linearly implicit scheme for solving the coupled nonlinear Schrödinger equations was developed in [Ismail and Taha (2007)]. The new six-point scheme for solving the coupled nonlinear Schrödinger system is proposed to study the collision behaviors of the soliton waves in [Sun, Gu, and Ma (2004)]. Author of [Ismail (2008a)] developed a fourth-order finite difference scheme in both directions i.e. space and time variables for solving coupled nonlinear Schrödinger equations. Also see [Ismail (2008b)]. Five methods for the integration in time of a semi-discretization of the nonlinear Schrödinger equation are extensively tested in [Sanz-Serna and Verwer (1986)]. The solution of coupled nonlinear Schrödinger equations based on pseudospectral collocation method with domain decomposition algorithm for approximating the spatial variable was proposed in [Dehghan and Taleei (2011)]. In [Kol and Wofo (2013)] the (G'/G) -expansion method is used for solving a system of two coupled discrete nonlinear Schrödinger equations with a saturable nonlinearity. Authors of [Fei, Perez-Garcia, and Vazquez (1995)] proposed conservative finite difference scheme for nonlinear Schrödinger systems. The new scheme shows some clear advantages over the previously proposed integration methods. Authors of [de la Hoz and Vadillo (2008)] studied the exponential time differencing fourth-order Runge-Kutta (ETDRK4) method for solving a wide range of nonlinear wave equations such as Burger's, one and two-dimensional nonlinear Schrödinger equations. Authors of [Cox and Matthews (2002)] studied and tested a class of numerical methods for systems with stiff linear parts, based on combining exponential time differencing for the linear terms with a method similar to Adams-Bashforth for the nonlinear terms. Authors of [Zhang, Meng, Xu, Li, and Tian (2007)] presented the Hirota method and symbolic computation for obtaining the analytical bright one and two-soliton solutions of the (2+1)-dimensional CNLS equations under certain constraints.

1.3 A brief review of the meshless method

In recent years radial basis functions (RBFs) have been extensively used in different context and emerged as a potential alternative in the field of numerical solution of PDEs. The use of RBFs in the numerical solution of partial differential equations (PDEs) has gained popularity in engineering and science community as it

is meshless and can readily be extended to multi-dimensional problems. A truly meshless method, called the Meshless Local Petrov-Galerkin (MLPG) method was discussed in depth in [Atluri (2004)]. A local symmetric weak form (LSWF) for linear potential problems is developed, and a truly meshless method, based on the LSWF and the moving least squares approximation, is presented for solving potential problems with high accuracy in [Atluri and Zhu (1998)]. Authors of [Atluri and Shen (2002)] studied the efficiency and accuracy of a variety of meshless trial and test functions based on the general concept of the meshless local Petrov-Galerkin (MLPG) method. Five types of trial functions, and six types of test functions are introduced in [Atluri and Shen (2002)]. The key idea of the meshless methods is that they can obtain accurate and stable solutions of integral equations or partial differential equations with various boundary conditions with a set of particles without using any mesh [Mirzaei and Dehghan (2010a)]. Authors of [Mirzaei and Dehghan (2010b)] presented the MLPG method for numerically solving the non-linear two-dimensional sine-Gordon (SG) equation. Authors of [Abbasbandy and Shirzadi (2011)] presented a new approach based on the meshless local Petrov-Galerkin (MLPG) and collocation methods to treat the parabolic partial differential equations with Neumann and non-classical boundary conditions. A meshless local Petrov-Galerkin (MLPG) method is applied in [Sladek, Sladek, Krivacek, Wen, and Zhang (2007)] to solve dynamic plate bending problems described by the Reissner-Mindlin theory. The meshless local Petrov-Galerkin (MLPG) method is used in [Sladek, Sladek, and Hon (2006)] to solve stationary and transient heat conduction inverse problems in 2-D and 3-D axisymmetric bodies. Authors of [Sladek, Sladek, Zhang, and Schanz (2006)] employed a meshless method based on the local Petrov-Galerkin approach for the numerical solution of quasistatic and transient dynamic problems in two-dimensional (2D) nonhomogeneous linear viscoelastic media. Also see [Abbasbandy, Ghehsareh, Alhuthali, and Alsulami (2014)]. The most important advantages of meshless methods compared to finite element methods are: their high-order continuous shape functions, simpler incorporation of h- and p-adaptivity and certain advantages in crack problems.

Recently, many fractional partial differential equations are solved using meshless approach based on the radial basis functions and moving least squares (MLS) approximation. In [Gu, Zhuang, and Liu (2011)] authors presented an implicit meshless collocation technique for solving time-fractional diffusion equation. Also, the stability and convergence of this meshless method are investigated theoretically and numerically in [Gu, Zhuang, and Liu (2011)]. Authors of [Gu, Zhuang, and Liu (2010)] presented an implicit meshless technique based on the radial basis functions for the numerical simulation of the anomalous sub-diffusion equation.

Also, they discussed the stability and convergence of their method. Authors of [Liu, Gu, Zhuang, Liu, and Nie (2011)] presented an implicit meshless method based on the radial basis functions for the numerical simulation of time-fractional diffusion equation. Authors of [Zhuang, Liu, Anh, and Turner (2008)] presented an implicit meshless approach based on the moving least squares (MLS) approximation for the numerical simulation of fractional advection-diffusion equation. Authors of [Mohebbi, Abbaszadeh, and Dehghan (2013)] proposed a numerical method for the solution of the time-fractional nonlinear Schrödinger equation in one and two dimensions which appears in quantum mechanics. The meshless method has already proved successful in standard quantum mechanics as well as for several other engineering and physical problems [Abbasbandy, Ghehsareh, and Hashim (2013); Dehghan and Salehi (2011); Dehghan and Tatari (2008); Dehghan and Nikpour (2013); Tatari and Dehghan (2010)]. The aim of the current paper is to show that the meshless methods based on the radial basis functions and collocation approach and also meshless local Petrov-Galerkin technique [Sladek, Stanak, Han, Sladek, and Atluri (2013)] are also suitable for the treatment of some nonlinear partial differential equations.

1.4 The main aim and structure of this paper

In this paper, in case of one-dimensional, we apply the RBFs collocation meshless method for the solution of Eq. (1) and in case of two-dimensional, we use meshless local Petrov-Galerkin approach and local RPIM for obtaining two numerical algorithms to solve Eq. (1). Firstly, we obtain a time semi-discretization scheme using the forward finite difference formula. In case of one dimension, we build a full discretization scheme using the meshless method based on radial basis functions (RBFs) and Kansa's approach. Then, in case of two-dimension using time discrete scheme, we obtain a local weak form. Now, in the local weak form, we have two space functions that one of them is test function and another is trial function. In our meshless local weak form, the test functions are weight functions of moving least squares approximation but the trial functions in the MLPG [Salehi and Dehghan (2014)] and LRPIM methods [Dehghan and Ghesmati (2010)] are shape functions of MLS and shape functions of RPIM, respectively. The aim of this paper is to show that the meshless method based on the radial basis functions and collocation approach is also suitable for the treatment of system of coupled nonlinear partial differential equations.

The outline of this paper is as follows. In Section 2 we explain the basic concepts of RBFs approximation method. In Section 3, we introduce the system of 4-coupled nonlinear Schrödinger equations and obtain a time discrete scheme which employs

the forward finite difference formula and implements the RBFs meshless collocation method. Also, in Section 4, we explain the system of 2-coupled nonlinear Schrödinger equations and obtain a time discrete technique using forward finite difference scheme and a full discretization scheme using RBFs meshless method. The two-dimensional coupled damped nonlinear system of Schrödinger equations is introduced in Section 5. Also, we present a time discrete scheme using the forward finite difference formula and obtain a full discretization scheme using RBFs meshless method for the model introduced in this section. The MLS approximation and RPIM and their shape functions for the MLPG and LRPIM methods are introduced in Section 5. Also, in this section we explain how to implement the MLPG and LRPIM methods for solving the mentioned model. In Section 6 we solve several test problems and report some numerical simulations. Finally a conclusion is given in Section 7.

2 Basic concepts for RBFs approximation method

As mentioned in [Liu and Gu (2005)] the definition of a meshfree method is:

A meshfree method is a method used to establish system algebraic equations for the whole problem domain without the use of a predefined mesh for the domain discretization.

Also, as said in [Liu and Gu (2005)] meshfree methods use a set of nodes scattered within the problem domain as well as sets of nodes scattered on the boundaries of the domain to represent (not discretize) the problem domain and its boundaries. These sets of scattered nodes are called field nodes, and they do not form a mesh, meaning it does not require any a priori information on the relationship between the nodes for the interpolation or approximation of the unknown functions of field variables. In this paper, we use the meshfree method based on RBFs collocation approach. The reason we use the RBFs collocation method is that it works for arbitrary geometry with high dimensions and it does not require a mesh at all. The meshfree method using RBFs is the so-called Kansa's method [Kansa (1990b);Kansa (1990a);Kansa, Aldredge, and Ling (2009)], where the RBFs are directly implemented for the approximation of the solution of PDEs. Kansa's method was developed in 1990, in which the concept of solving PDEs by using RBFs, especially MQ, was initiated. As mentioned in [Vanani and Aminataei (2008)], the MQ approximation scheme was first introduced by Hardy [Hardy (1971)] who successfully applied this method for approximating surface and bodies from field data. In this section we introduce the basic definitions of radial basis functions in the general case and we express some basic theorems for the interpolation error using

the radial basis functions.

Definition 1. [Wendland (2005)] A symmetric function $\phi \in \mathbb{R}^d \times \mathbb{R}^d \rightarrow \mathbb{R}$ is strictly conditionally positive definite of order m , if for all sets $X = \{x_1, \dots, x_N\} \subset \mathbb{R}^d$ of distinct points, and all vectors $\lambda \in \mathbb{R}^d$ satisfying $\sum_{i=1}^N \lambda_i p(x_i) = 0$ for any polynomial p of degree at most $m - 1$, the quadratic form

$$\lambda^T A \lambda = \sum_{i=1}^N \sum_{j=1}^N \lambda_i \lambda_j \phi(x_i - x_j),$$

is positive, whenever $\lambda \neq 0$.

We interpolate a continuous function $f : \mathbb{R}^d \rightarrow \mathbb{R}$ on a set $X = \{x_1, \dots, x_N\}$ with choosing the radial basis function for $\phi : \mathbb{R}^d \rightarrow \mathbb{R}$ that is radial in the sense that $\phi(x) = \Psi(\|x\|)$, where $\|\cdot\|$ is the usual Euclidean norm on \mathbb{R}^d as we will explain in the next section. Now, we assume ϕ to be strictly conditionally positive definite of order m , then the interpolation function has the following form

$$\mathcal{I}f(x) = \sum_{i=1}^N \lambda_i \phi(x - x_i) + \sum_{j=1}^l \gamma_j p_j(x),$$

where $l = \binom{d+m-1}{m-1}$ and $\{p_1, p_2, \dots, p_l\}$ is a basis of Π_m^d . The basis problem is to find $N + l$ unknown coefficients λ_i and γ_j in which N interpolation conditions are to the following form

$$\mathcal{I}f(x_i) = f_i, \quad i = 1, \dots, N,$$

and for l remaining conditions we use the following equations

$$\sum_{i=1}^N \lambda_i p_j(x_i) = 0, \quad 1 \leq j \leq l.$$

Definition 2.[Wendland (2005)] The shifted surface splines are defined as

$$\phi(x) = \begin{cases} (-1)^{\lceil m - \frac{d}{2} \rceil} (x^2 + c^2)^{m - \frac{d}{2}}, & d \text{ odd}, \\ (-1)^{m - \frac{d}{2} + 1} (x^2 + c^2)^{m - \frac{d}{2}} \log \sqrt{x^2 + c^2}, & d \text{ even}, \end{cases}$$

where $d, m \in \mathbb{N}$ and $m > d/2$.

Definition 3.[Wendland (2005)] The density of X in Ω is the number

$$h = h(\Omega, X) = \sup_{x \in \Omega} \min_{x_j \in X} |x - x_j|.$$

Theorem 3.[Kazemi and Ghoreishi (2013);Wendland (2005)] Suppose that $\phi \in C(\mathbb{R}^d)$ is an even conditionally positive definite function of order m and has a continuous generalized transform $\hat{\phi}$ of order m on $\mathbb{R}^d \setminus \{0\}$. Let \mathcal{F}_ϕ be the real vector space consisting of all functions $f \in C(\mathbb{R}^d)$ that are slowly increasing and have a generalized Fourier transform \hat{f} of order $m/2$ that satisfies $\frac{\hat{f}}{\sqrt{\hat{\phi}}} \in L_2(\mathbb{R}^d)$. Equip \mathcal{F}_ϕ with the symmetric bilinear form

$$(f, g)_\phi = \frac{1}{(2\pi)^{d/2}} \int_{\mathbb{R}^d} \frac{\hat{f}(\eta)\overline{\hat{g}(\eta)}}{\hat{\phi}(\eta)} d\eta.$$

Then for the given basis function ϕ , function space \mathcal{F}_ϕ is called the *native* space for ϕ , with semi-norm $|\cdot|_\phi$.

Now, we assume that domain Ω has Lipschitz boundary [Dacorogna (2004)] and also has the uniform interior cone property [Wendland (2005)]. Approximation function error bound in radial basis functions interpolation can be estimated using the following theorem.

Theorem 4.[Yoon (2003)] Let $\mathcal{I}f(x)$ be an interpolant of f on X using radial basis function ϕ in Definition 3 and f be a function in the space \mathcal{F}_ϕ . Then for every function $f \in W_2^m$ we have

$$|f - \mathcal{I}f|_{m,2} \leq |f - \mathcal{I}f|_\phi \leq |f|_\phi.$$

Also, as mentioned in [Mohyud-Din, Negahdary, and Usman (2012)], the exponential convergence proof in applying RBFs in Sobolov space is given by Yoon [Yoon (1999)], spectral convergence of the method in the limit of flat RBFs is shown by Fornberg et al. [Fornberg, Wright, and Larsson (2004)]. Some popular choices of RBFs [Shokri and Dehghan (2010)] are listed in the following table where the free parameter c is called the shape parameter [Shokri and Dehghan (2012)] of the RBFs.

Name of function	Definition
Linear	r
Cubic	r^3
Multiquadratics(MQ)	$\sqrt{r^2 + c^2}$
Gaussian(GS)	e^{-cr^2}
polyharmonic splines	$r^{2n} \ln(r), r^{2n-1}$

A mentioned in [Rippa (1999)] the accuracy of many schemes for interpolating scattered data with radial basis functions depends on a shape parameter, c , of the radial basis function. Author of [Rippa (1999)] showed, numerically, that the optimal value of c depends on the number and distribution of data points, on the data vector, and on the precision of the computation and he presented an algorithm for selecting a good value for c that implicitly takes all the above considerations into account [Rippa (1999)]. Also, authors of [Huang, Yen, and Cheng (2010)] showed, numerically, that RBFs in fact perform better than polynomials, as the optimal shape parameter exists not in the limit, but at a finite value.

3 System of 4-coupled nonlinear Schrödinger equations

We consider system of four coupled nonlinear Schrödinger equations under the assumptions $0 \leq t \leq T$ and $X_L \leq x \leq X_R$.

3.1 Time discretization

We presented a spatial discretization procedure for system (1) for $N = 4$. We put $\alpha_n = \frac{1}{\mu}$, $\sigma_{nm} = \sigma$, $n = 1, 2, 3, 4$, and $\sigma_{nm} = e$, $n \neq m$ in system (1) for $N = 4$ so that, for our numerical study we consider the following system [Bhatt and Khaliq (2014)]:

$$\left\{ \begin{aligned} i \frac{\partial \Psi_1}{\partial t} + \frac{1}{\mu} \frac{\partial^2 \Psi_1}{\partial x^2} + \left[\sigma |\Psi_1|^2 + e \left(|\Psi_2|^2 + |\Psi_3|^2 + |\Psi_4|^2 \right) \right] \Psi_1 &= 0, \\ i \frac{\partial \Psi_2}{\partial t} + \frac{1}{\mu} \frac{\partial^2 \Psi_2}{\partial x^2} + \left[\sigma |\Psi_2|^2 + e \left(|\Psi_1|^2 + |\Psi_3|^2 + |\Psi_4|^2 \right) \right] \Psi_2 &= 0, \\ i \frac{\partial \Psi_3}{\partial t} + \frac{1}{\mu} \frac{\partial^2 \Psi_3}{\partial x^2} + \left[\sigma |\Psi_3|^2 + e \left(|\Psi_1|^2 + |\Psi_2|^2 + |\Psi_4|^2 \right) \right] \Psi_3 &= 0, \\ i \frac{\partial \Psi_4}{\partial t} + \frac{1}{\mu} \frac{\partial^2 \Psi_4}{\partial x^2} + \left[\sigma |\Psi_4|^2 + e \left(|\Psi_1|^2 + |\Psi_2|^2 + |\Psi_3|^2 \right) \right] \Psi_4 &= 0, \end{aligned} \right. \tag{4}$$

with initial condition

$$\Psi_n(x, 0) = g_n(x), \quad n = 1, 2, 3, 4, \tag{5}$$

and assume that we have no flux boundary conditions

$$\frac{\partial \Psi_n(x, t)}{\partial x} = 0, \quad n = 1, 2, 3, 4, \quad \text{at } x = x_L, x_R, \quad t \geq 0. \tag{6}$$

For discretization of time variable, we need some preliminary. We define

$$t_k = k\tau, \quad k = 0, 1, \dots, N_T,$$

where $\tau = T/N_T$ is the step size of time variable. In this section, we discretize the time variable using the forward finite difference procedure for the first-order derivative on time variable. We consider Eq. (4) in point (x, t_n) , then we have

$$\begin{cases} i\Psi_1^n + \frac{\tau}{\mu} \frac{\partial^2 \Psi_1^n}{\partial x^2} = i\Psi_1^{n-1} - \tau \left[\sigma |\Psi_1^{n-1}|^2 + e \left(|\Psi_2^{n-1}|^2 + |\Psi_3^{n-1}|^2 + |\Psi_4^{n-1}|^2 \right) \right] \Psi_1^{n-1}, \\ i\Psi_2^n + \frac{\tau}{\mu} \frac{\partial^2 \Psi_2^n}{\partial x^2} = i\Psi_2^{n-1} - \tau \left[\sigma |\Psi_2^{n-1}|^2 + e \left(|\Psi_1^{n-1}|^2 + |\Psi_3^{n-1}|^2 + |\Psi_4^{n-1}|^2 \right) \right] \Psi_2^{n-1}, \\ i\Psi_3^n + \frac{\tau}{\mu} \frac{\partial^2 \Psi_3^n}{\partial x^2} = i\Psi_3^{n-1} - \tau \left[\sigma |\Psi_3^{n-1}|^2 + e \left(|\Psi_1^{n-1}|^2 + |\Psi_2^{n-1}|^2 + |\Psi_4^{n-1}|^2 \right) \right] \Psi_3^{n-1}, \\ i\Psi_4^n + \frac{\tau}{\mu} \frac{\partial^2 \Psi_4^n}{\partial x^2} = i\Psi_4^{n-1} - \tau \left[\sigma |\Psi_4^{n-1}|^2 + e \left(|\Psi_1^{n-1}|^2 + |\Psi_2^{n-1}|^2 + |\Psi_3^{n-1}|^2 \right) \right] \Psi_4^{n-1}. \end{cases} \quad (7)$$

3.2 Implementation of RBFs meshless method

We assume that, Ω is an arbitrary interval in \mathbf{R} . The approximate expansion of $u(x_k, t_n)$ form $p = 1, 2, 3, 4$, is as follows

$$\Psi_p(x_k, t_n) = \sum_{j=1}^M c_{j,(p)}^n \varphi(r_{kj}), \quad (8)$$

in which

$$\varphi(r_{kj}) = \sqrt{(x_k - x_j)^2 + c^2} = \sqrt{r^2 + c^2}.$$

For the use of Kansa's method, we let $\{x_k\}_{k=1}^M$ be M collocation points in Ω in which $\{x_k\}_{k=2}^{M-1}$ are interior points and $\{x_k\}_{k=1,M}$ are boundary points. For each point x_k , let us denote

$$\varphi_j(x) = \sqrt{(x - x_j)^2 + c^2}.$$

Substituting (8) into (6) and (7) results the following matrix form

$$\mathbf{AC}^n = \mathbf{B}^n,$$

in which the coefficient matrix is to the following form

$$\begin{bmatrix} (A_1)_{M \times M} & 0 & 0 & 0 \\ 0 & (A_2)_{M \times M} & 0 & 0 \\ 0 & 0 & (A_3)_{M \times M} & 0 \\ 0 & 0 & 0 & (A_4)_{M \times M} \end{bmatrix}_{4M \times 4M},$$

where for $p = 1, 2, 3, 4$,

$$\begin{cases} (A_p)_{i,j} = \frac{\partial \varphi(r_{ij})}{\partial x}, & i = 1, M, \quad j = 1, 2, \dots, M, \\ (A_p)_{i,j} = i\varphi(r_{ij}) + \frac{\tau}{\mu} \frac{\partial^2 \varphi(r_{ij})}{\partial x^2}, & i = 2, \dots, M-1, \quad j = 1, 2, \dots, M. \end{cases}$$

Also, \mathbf{C}^n and \mathbf{B}^n are

$$\mathbf{C}^n = \left[\underbrace{c_{1,(1)}^n, c_{2,(1)}^n, \dots, c_{M,(1)}^n}_{p=1}, \underbrace{c_{1,(2)}^n, c_{2,(2)}^n, \dots, c_{M,(2)}^n}_{p=2}, \underbrace{c_{1,(3)}^n, c_{2,(3)}^n, \dots, c_{M,(3)}^n}_{p=3}, \underbrace{c_{1,(4)}^n, c_{2,(4)}^n, \dots, c_{M,(4)}^n}_{p=4} \right]^T$$

$$\mathbf{B}^n = \left[\underbrace{b_{1,(1)}, b_{2,(1)}, \dots, b_{M,(1)}}_{p=1}, \underbrace{b_{1,(2)}, b_{2,(2)}, \dots, b_{M,(2)}}_{p=2}, \underbrace{b_{1,(3)}, b_{2,(3)}, \dots, b_{M,(3)}}_{p=3}, \underbrace{b_{1,(4)}, b_{2,(4)}, \dots, b_{M,(4)}}_{p=4} \right]^T$$

in which

$$\begin{cases} b_{k,(p)} = 0, & k = 1, M, \quad p = 1, 2, 3, 4, \\ b_{r,(p)} = i \sum_{j=1}^M c_{j(p)}^{n-1} \varphi(r_{rj}) - \tau \left[\sigma \left| \sum_{j=1}^M c_{j(p)}^{n-1} \varphi(r_{rj}) \right|^2 + e \left(\sum_{\substack{q=1 \\ q \neq p}}^4 \left| \sum_{j=1}^M c_{j(q)}^{n-1} \varphi(r_{rj}) \right|^2 \right) \right] \times \sum_{j=1}^M c_{j(p)}^{n-1} \varphi(r_{rj}), \\ r = 2, 3, \dots, M-2, M-1, \quad p = 1, 2, 3, 4. \end{cases}$$

After solving the algebraic system of equations $\mathbf{AC}^n = \mathbf{B}^n$ at each time step, we can construct the solution using the approximation (8). Also, the coefficient matrix is ill-conditioned, therefore, we use the LU decomposition method for solving linear system of algebraic equations $\mathbf{AC}^n = \mathbf{B}^n$.

4 System of 2-coupled nonlinear Schrödinger equations

We consider system of 2-coupled nonlinear Schrödinger equations under the assumptions $0 \leq t \leq T$ and $X_L \leq x \leq X_R$. In this section, we solve system (1) for $N = 2$ with $\alpha_1 = \alpha_2 = \frac{1}{\mu}$ which is to the following form [Bhatt and Khaliq (2014)]

$$\begin{cases} i \frac{\partial \Psi_1}{\partial t} + \frac{1}{\mu} \frac{\partial^2 \Psi_1}{\partial x^2} + [\sigma_{11} |\Psi_1|^2 + \sigma_{12} |\Psi_2|^2] \Psi_1 = 0, \\ i \frac{\partial \Psi_2}{\partial t} + \frac{1}{\mu} \frac{\partial^2 \Psi_2}{\partial x^2} + [\sigma_{21} |\Psi_1|^2 + \sigma_{22} |\Psi_2|^2] \Psi_2 = 0, \end{cases} \quad x_L \leq x \leq x_R, \tag{9}$$

in which in the case of single soliton with the initial conditions we have

$$\begin{aligned} \Psi_1(x, 0) &= \sqrt{\frac{\mu \alpha}{1+e}} \operatorname{sech}(\sqrt{\mu \alpha} x) e^{i \nu x}, \\ \Psi_2(x, 0) &= \sqrt{\frac{\mu \alpha}{1+e}} \operatorname{sech}(\sqrt{\mu \alpha} x) e^{i \nu x}, \end{aligned} \tag{10}$$

and in the case of interaction of two solitons with the initial conditions we have

$$\begin{cases} \Psi_1(x, 0) = \sqrt{2} r_1 \operatorname{sech}(r_1 x + x_0) \exp(i \nu_1 x), \\ \Psi_2(x, 0) = \sqrt{2} r_2 \operatorname{sech}(r_2 x + x_1) \exp(i \nu_2 x), \end{cases} \tag{11}$$

and boundary conditions

$$\frac{\partial \Psi_1(x, t)}{\partial x} = \frac{\partial \Psi_2(x, t)}{\partial x} = 0, \quad x = x_L, x_R, \quad t \geq 0, \tag{12}$$

where $\alpha, \nu, r_1, r_2, x_0, x_1$ and e are constants.

4.1 Time discretization

We presented a spatial discretization procedure for system (9) for $N = 2$. For discretization of time variable, we need some preliminary. We define

$$t_k = k \tau, \quad k = 0, 1, \dots, N_T,$$

where $\tau = T/N_T$ is the step size of time variable. In this section, we discretize the time variable using the forward finite difference formula for the first-order deriva-

tive on time variable. We consider Eq. (9) at point (x, t_n) , then we have

$$\begin{cases} i\Psi_1^n + \frac{\tau}{\mu} \frac{\partial^2 \Psi_1^n}{\partial x^2} = i\Psi_1^{n-1} - \tau \left[\sigma_{11} |\Psi_1^{n-1}|^2 + \sigma_{12} |\Psi_2^{n-1}|^2 \right] \Psi_1^{n-1}, \\ i\Psi_2^n + \frac{1}{\mu} \frac{\partial^2 \Psi_2^n}{\partial x^2} = i\Psi_2^{n-1} - \tau \left[\sigma_{21} |\Psi_1^{n-1}|^2 + \sigma_{22} |\Psi_2^{n-1}|^2 \right] \Psi_2^{n-1}. \end{cases} \quad (13)$$

4.2 Implementation of RBFs meshless method

We assume that, Ω is an arbitrary interval in \mathbf{R} . The approximate expansion of $u(x_k, t_n)$ form $p = 1, 2$, is as follows

$$\Psi_p(x_k, t_n) = \sum_{j=1}^M c_{j,(p)}^n \varphi(r_{kj}), \quad (14)$$

in which

$$\varphi(r_{kj}) = \sqrt{(x_k - x_j)^2 + c^2} = \sqrt{r^2 + c^2}.$$

For the use of Kansa’s method, we let $\{x_k\}_{k=1}^M$ be M collocation points in Ω in which $\{x_k\}_{k=2}^{M-1}$ are interior points and $\{x_k\}_{k=1, M}$ are boundary points. For each point x_k , let us denote

$$\varphi_j(x) = \sqrt{(x - x_j)^2 + c^2}.$$

Substituting (14) into (12) and (13) results the following matrix form

$$\mathbf{AC}^n = \mathbf{B}^n,$$

in which the coefficient matrix is to the following form

$$\begin{bmatrix} (A_1)_{M \times M} & 0 \\ 0 & (A_2)_{M \times M} \end{bmatrix}_{2M \times 2M},$$

where for $p = 1, 2$,

$$\begin{cases} (A_p)_{i,j} = \frac{\partial \varphi(r_{ij})}{\partial x}, \quad i = 1, M, \quad j = 1, 2, \dots, M, \\ (A_p)_{i,j} = i\varphi(r_{ij}) + \frac{\tau}{\mu} \frac{\partial^2 \varphi(r_{ij})}{\partial x^2}, \quad i = 2, \dots, M-1, \quad j = 1, 2, \dots, M. \end{cases}$$

Also, \mathbf{C}^n and \mathbf{B}^n are

$$\mathbf{C}^n = \left[\underbrace{c_{1,(1)}^n, c_{2,(1)}^n, \dots, c_{M,(1)}^n}_{p=1}, \underbrace{c_{1,(2)}^n, c_{2,(2)}^n, \dots, c_{M,(2)}^n}_{p=2} \right]^T,$$

$$\mathbf{B}^n = \left[\underbrace{b_{1,(1)}, b_{2,(1)}, \dots, b_{M,(1)}}_{p=1}, \underbrace{b_{1,(2)}, b_{2,(2)}, \dots, b_{M,(2)}}_{p=2} \right]^T,$$

in which

$$\left\{ \begin{array}{l} b_{k,(p)} = 0, \quad k = 1, M, \quad p = 1, 2, \\ b_{r,(1)} = i \sum_{j=1}^M c_{j(1)}^{n-1} \varphi(r_{rj}) - \tau \left[\sigma_{11} \left| \sum_{j=1}^M c_{j(1)}^{n-1} \varphi(r_{rj}) \right|^2 + \sigma_{12} \left| \sum_{j=1}^M c_{j(2)}^{n-1} \varphi(r_{rj}) \right|^2 \right] \times \sum_{j=1}^M c_{j(1)}^{n-1} \varphi(r_{rj}), \\ b_{r,(2)} = i \sum_{j=1}^M c_{j(2)}^{n-1} \varphi(r_{rj}) - \tau \left[\sigma_{21} \left| \sum_{j=1}^M c_{j(1)}^{n-1} \varphi(r_{rj}) \right|^2 + \sigma_{22} \left| \sum_{j=1}^M c_{j(2)}^{n-1} \varphi(r_{rj}) \right|^2 \right] \times \sum_{j=1}^M c_{j(2)}^{n-1} \varphi(r_{rj}), \\ r = 2, 3, \dots, M-2, M-1. \end{array} \right.$$

After solving the algebraic system of equations $\mathbf{AC}^n = \mathbf{B}^n$ at each time step, we can construct the solution using the approximation (8). Also, the coefficient matrix is ill-conditioned, therefore, we use the LU decomposition method for solving linear system of algebraic equations $\mathbf{AC}^n = \mathbf{B}^n$.

5 The two-dimensional coupled damped nonlinear system of Schrödinger equations

We consider the coupled damped nonlinear system of Schrödinger equations with additional convection term (CDNSEC) of the form [Asadzadeh, Rostamy, and Zabihi (2013)]

$$\left\{ \begin{array}{l} i \frac{\partial \Psi_1}{\partial t} + \beta \cdot \nabla \Psi_1 + \frac{1}{2} \Delta \Psi_1 + \varepsilon \left(|\Psi_1|^2 + \alpha |\Psi_2|^2 \right) \Psi_1 = 0, \\ i \frac{\partial \Psi_2}{\partial t} + \beta \cdot \nabla \Psi_2 + \frac{1}{2} \Delta \Psi_2 + \varepsilon \left(\alpha |\Psi_1|^2 + |\Psi_2|^2 \right) \Psi_2 = 0, \\ (x, t) \in \Omega \times [0, T], \end{array} \right. \tag{15}$$

with initial conditions

$$\Psi_1(x, 0) = g_1(x), \quad \Psi_2(x, 0) = g_2(x), \quad x \in \Omega, \tag{16}$$

and boundary conditions

$$\nabla\Psi_1(x, t) = \nabla\Psi_2(x, t) = 0, \quad \forall x \in \{x \in \partial\Omega : \mathbf{n}(x) \cdot \boldsymbol{\beta} < 0\}, \tag{17}$$

where $\mathbf{n}(x)$ is the outward unit normal to $\partial\Omega$ at the point $x \in \partial\Omega$. We assume that the solution of the system (15) is negligibly small outside the d -dimensional domain $[x_L, x_R]^d$.

5.1 Time discretization

We presented a spatial discretization procedure for system (9) for $N = 2$. For discretization of time variable, we present some preliminary. We define

$$t_k = k\tau, \quad k = 0, 1, \dots, N_T,$$

where $\tau = T/N_T$ is the step size of time variable. In this section, we discretize the time variable using the forward finite difference technique for the first-order derivative on time variable. We consider Eq. (15) at point (x, t_n) , then we obtain

$$\begin{cases} i\Psi_1^n + \tau\boldsymbol{\beta} \cdot \nabla\Psi_1^n + \frac{\tau}{2}\Delta\Psi_1^n = i\Psi_1^{n-1} - \tau\varepsilon \left(|\Psi_1^{n-1}|^2 + \alpha|\Psi_1^{n-1}|^2 \right) \Psi_1^{n-1}, \\ i\Psi_2^n + \tau\boldsymbol{\beta} \cdot \nabla\Psi_2^n + \frac{\tau}{2}\Delta\Psi_2^n = i\Psi_2^{n-1} - \tau\varepsilon \left(\alpha|\Psi_1^{n-1}|^2 + |\Psi_2^{n-1}|^2 \right) \Psi_2^{n-1}. \end{cases} \tag{18}$$

5.2 Implementation of RBFs meshless method

In this case, Ω is an arbitrary interval in \mathbf{R} . The approximate expansion of $u(x_k, t_n)$ for $p = 1, 2$, is as follows

$$\Psi_p(x_k, t_n) = \sum_{j=1}^M c_{j,(p)}^n \varphi(r_{kj}), \tag{19}$$

in which

$$\varphi(r_{kj}) = \sqrt{(\mathbf{x}_k - \mathbf{x}_j)^2 + c^2} = \sqrt{r^2 + c^2}.$$

For the use of Kansa’s method, we let $\{\mathbf{x}_k\}_{k=1}^M$ be M collocation points in Ω in which $\{\mathbf{x}_k\}_{k=M_B+1}^M$ are interior points and $\{\mathbf{x}_k\}_{k=1}^{M_B}$ are boundary points. For each point x_k , let us denote

$$\varphi_j(\mathbf{x}) = \sqrt{(\mathbf{x} - \mathbf{x}_j)^2 + c^2}.$$

Now substituting (19) into (17) and (18) results the following matrix form

$$\mathbf{AC}^n = \mathbf{B}^n,$$

in which the coefficient matrix is to the following form

$$\begin{bmatrix} (A_1)_{M \times M} & \mathbf{0} \\ \mathbf{0} & (A_2)_{M \times M} \end{bmatrix}_{2M \times 2M},$$

where for $p = 1, 2$, we can write

$$\begin{cases} (A_p)_{i,j} = \nabla \varphi(r_{ij}), & i = 1, 2, \dots, M_B, \quad j = 1, 2, \dots, M, \\ (A_p)_{i,j} = i\varphi(r_{ij}) + \tau\beta \cdot \nabla \varphi(r_{ij}) + \frac{\tau}{2} \Delta \varphi(r_{ij}), & i = M_B + 1, \dots, M, \quad j = 1, 2, \dots, M. \end{cases}$$

Also, \mathbf{B}^n and \mathbf{C}^n are

$$\mathbf{B}^n = \left[\underbrace{b_{1,(1)}, b_{2,(1)}, \dots, b_{M,(1)}}_{p=1}, \underbrace{b_{1,(2)}, b_{2,(2)}, \dots, b_{M,(2)}}_{p=2} \right]^T,$$

$$\mathbf{C}^n = \left[\underbrace{c_{1,(1)}^n, c_{2,(1)}^n, \dots, c_{M,(1)}^n}_{p=1}, \underbrace{c_{1,(2)}^n, c_{2,(2)}^n, \dots, c_{M,(2)}^n}_{p=2} \right]^T,$$

in which

$$\begin{cases} b_{k,(p)} = 0, & k = 1, 2, \dots, M_B, \quad p = 1, 2, \\ b_{r,(1)} = i \sum_{j=1}^M c_{j(1)}^{n-1} \varphi(r_{rj}) - \tau \varepsilon \left[\left| \sum_{j=1}^M c_{j(1)}^{n-1} \varphi(r_{rj}) \right|^2 + \alpha \left| \sum_{j=1}^M c_{j(2)}^{n-1} \varphi(r_{rj}) \right|^2 \right] \times \sum_{j=1}^M c_{j(1)}^{n-1} \varphi(r_{rj}), \\ b_{r,(2)} = i \sum_{j=1}^M c_{j(2)}^{n-1} \varphi(r_{rj}) - \tau \varepsilon \left[\alpha \left| \sum_{j=1}^M c_{j(1)}^{n-1} \varphi(r_{rj}) \right|^2 + \left| \sum_{j=1}^M c_{j(2)}^{n-1} \varphi(r_{rj}) \right|^2 \right] \times \sum_{j=1}^M c_{j(2)}^{n-1} \varphi(r_{rj}), \\ r = M_B + 1, \dots, M. \end{cases}$$

After solving the algebraic system of equations $\mathbf{AC}^n = \mathbf{B}^n$ at each time step, we can construct the solution using (19). Also, the coefficient matrix is ill-conditioned, therefore, we use the LU decomposition method for solving linear system of algebraic equations $\mathbf{AC}^n = \mathbf{B}^n$.

5.3 Shape function of radial point interpolation method (RPIM)

This subsection is taken from book of Liu and Gu [Liu and Gu (2005)]. The radial point interpolation method (RPIM) shape functions are used for meshless weak form and strong form methods. An approximation of unknown function u is as follows

$$u(\mathbf{x}) = \sum_{i=1}^n \mathbf{b}_i R_i(\mathbf{x}) + \sum_{j=1}^m \theta_j p_j(\mathbf{x}) = \mathbf{R}^T(\mathbf{x})\mathbf{b} + \mathbf{p}^T(\mathbf{x})\theta, \quad (20)$$

where $R_i(\mathbf{x})$ is a radial basis function (RBF), n is number of RBFs, $p_j(\mathbf{x})$ is polynomial in the Cartesian space $\mathbf{x}^T = [x, y]$ and m is number of polynomial basis functions. Also, coefficient \mathbf{b}_i and θ_j must be computed. For evaluating \mathbf{b}_i and θ_j in Eq. (10), we consider a support domain for the point of interest at \mathbf{x} in which n field nodes are located inside of this support domain. Collocating Eq. (10) in these n nodes we obtain the following matrix form

$$\mathbf{U}_s = \mathbf{R}_0 \mathbf{b} + \mathbf{P}_m \theta, \quad (21)$$

where \mathbf{U}_s is the vector of function values as follows

$$\mathbf{U}_s = [u_1 \ u_2 \ \dots \ u_n]^T. \quad (22)$$

The moment matrix of RBFs is

$$\mathbf{R}_0 = \begin{bmatrix} R_1(r_1) & R_2(r_1) & \dots & R_n(r_1) \\ R_1(r_2) & R_2(r_2) & & R_n(r_2) \\ \vdots & \vdots & \ddots & \vdots \\ R_1(r_n) & R_2(r_n) & \dots & R_n(r_n) \end{bmatrix}, \quad (23)$$

where r_k in $R_i(r_k)$ is $r_k = \sqrt{(x_k - x_i)^2 + (y_k - y_i)^2}$, and the polynomial moment matrix is

$$\mathbf{P}_m^T = \begin{bmatrix} 1 & 1 & \dots & 1 \\ x_1 & x_2 & \dots & x_n \\ y_1 & y_2 & \dots & y_n \\ \vdots & \vdots & \vdots & \vdots \\ p_m(x_1) & p_m(x_2) & \dots & p_m(x_n) \end{bmatrix}, \quad (24)$$

and also the vector of coefficients is to the following form

$$\mathbf{b}^T = [\mathbf{b}_1 \ \mathbf{b}_2 \ \dots \ \mathbf{b}_n]^T, \quad \theta^T = [\theta_1 \ \theta_2 \ \dots \ \theta_m]^T. \quad (25)$$

Here, There are $n + m$ number of unknown coefficients in Eq. (15), therefore, we need the additional m equations. So we can add the following m constraint conditions

$$\sum_{i=1}^n p_j(\mathbf{x}_i) \mathbf{b}_i = \mathbf{P}_m^T \mathbf{b} = 0, \quad j = 1, 2, \dots, m. \tag{26}$$

Considering Eqs. (15) and (26) we have the following vector-matrix form

$$\tilde{\mathbf{U}}_s = \begin{bmatrix} \mathbf{U}_s \\ 0 \end{bmatrix} = \begin{bmatrix} (\mathbf{R}_0)_{n \times n} & (\mathbf{P}_m)_{n \times m} \\ (\mathbf{P}_m^T)_{m \times n} & (\mathbf{0})_{m \times m} \end{bmatrix} \begin{bmatrix} \mathbf{b} \\ \boldsymbol{\theta} \end{bmatrix} = \mathbf{M} \mathbf{b}, \tag{27}$$

where

$$\mathbf{b}^T = [\mathbf{b}_1 \ \mathbf{b}_2 \ \dots \ \mathbf{b}_n \ \theta_1 \ \theta_2 \ \dots \ \theta_m], \tag{28}$$

$$\tilde{\mathbf{U}}_s = [u_1 \ u_2 \ \dots \ u_n \ 0 \ 0 \ \dots \ 0]. \tag{29}$$

Solving Eq. (27) to obtain the unknown coefficients arrives at

$$\mathbf{b} = \mathbf{M}^{-1} \tilde{\mathbf{U}}_s. \tag{30}$$

We consider Eq. (10) to the following form

$$u(\mathbf{x}) = \mathbf{R}^T(\mathbf{x}) \mathbf{b} + \mathbf{p}^T(\mathbf{x}) \boldsymbol{\theta} = [\mathbf{R}^T(\mathbf{x}) \ \mathbf{p}^T(\mathbf{x})] \begin{bmatrix} \mathbf{b} \\ \boldsymbol{\theta} \end{bmatrix}, \tag{31}$$

now using Eq. (30) we get

$$u(\mathbf{x}) = [\mathbf{R}^T(\mathbf{x}) \ \mathbf{p}^T(\mathbf{x})] \mathbf{M}^{-1} \tilde{\mathbf{U}}_s, \tag{32}$$

where the RPIM shape functions can be expressed as

$$\begin{aligned} \tilde{\Phi}(\mathbf{x}) &= [\mathbf{R}^T(\mathbf{x}) \ \mathbf{p}^T(\mathbf{x})] \mathbf{M}^{-1} \\ &= [\phi_1(x) \ \phi_2(x) \ \dots \ \phi_n(x) \ \phi_{n+1}(x) \ \phi_{n+2}(x) \ \dots \ \phi_{n+m}(x)]. \end{aligned} \tag{33}$$

So the RPIM shape functions corresponding to the nodal fields are

$$\Phi(\mathbf{x}) = [\phi_1(x) \ \phi_2(x) \ \dots \ \phi_n(x)]. \tag{34}$$

Finally, we have the following approximation

$$u(\mathbf{x}) = \Phi^T(\mathbf{x}) \mathbf{U}_s = \sum_{i=1}^n u(\mathbf{x}_i) \phi_i(\mathbf{x}). \tag{35}$$

5.4 Moving least squares (MLS) shape functions

This subsection is taken from book of Liu and Gu [Liu and Gu (2005)]. We consider an unknown scalar function of a field variable $u(\mathbf{x})$ in the domain Ω . The MLS approximation of $u(\mathbf{x})$ is defined at \mathbf{x} as

$$u_h(\mathbf{x}) = \sum_{j=1}^m p_j(\mathbf{x})\mathbf{a}_j(\mathbf{x}) = \mathbf{p}^T(\mathbf{x})\mathbf{a}(\mathbf{x}), \quad (36)$$

where $\mathbf{p}(\mathbf{x})$ is the basis function of the spatial coordinates and m is the number of the basis functions. When $\mathbf{p}(\mathbf{x}) = [x, y]^T$ we usually select the following basis functions

$$\mathbf{p}(\mathbf{x}) = [1, x, y], \quad \mathbf{p}(\mathbf{x}) = [1, x, y, xy, x^2, y^2],$$

also this basis function is built using monomials from the Pascal triangle to ensure minimum completeness. In Eq. (36), $\mathbf{a}(\mathbf{x})$ is the following vector of coefficients

$$\mathbf{a}^T(\mathbf{x}) = \{a_1(\mathbf{x}) \ a_2(\mathbf{x}) \ \cdots \ a_m(\mathbf{x})\}. \quad (37)$$

We can obtain the coefficient \mathbf{a} by minimizing the following weighted discrete L_2 -norm

$$J = \sum_{i=1}^M W(\mathbf{x} - \mathbf{x}_i) [\mathbf{p}^T(\mathbf{x}_i)\mathbf{a}(\mathbf{x}) - u_i]^2, \quad (38)$$

in which M is the number of nodes in the support domain of \mathbf{x} for which the weight function $W(\mathbf{x} - \mathbf{x}_i) \neq 0$ and u_i is value of u at $\mathbf{x} = \mathbf{x}_i$. The stationarity of J with respect to $\mathbf{a}(\mathbf{x})$ gives

$$\frac{\partial J}{\partial \mathbf{a}} = 0, \quad (39)$$

which leads to the following set of linear equations

$$\mathbf{A}(\mathbf{x})\mathbf{a}(\mathbf{x}) = \mathbf{B}(\mathbf{x})\mathbf{U}_s, \quad (40)$$

in which the vector \mathbf{U}_s is to the following form

$$\mathbf{U}_s = \{u_1 \ u_2 \ \cdots \ u_M\}, \quad (41)$$

and $\mathbf{A}(x)$ is called the weighted moment matrix defined as

$$\mathbf{A}(\mathbf{x}) = \sum_{i=1}^M W(\mathbf{x})\mathbf{p}(\mathbf{x}_i)\mathbf{p}(\mathbf{x}_i)^T. \quad (42)$$

Also the matrix \mathbf{B} in Eq. (40) is to the following form

$$\mathbf{B}(\mathbf{x}) = [W_1(\mathbf{x})\mathbf{p}(\mathbf{x}_1) \ W_2(x)\mathbf{p}(\mathbf{x}_2) \ \cdots \ W_M(\mathbf{x})\mathbf{p}(\mathbf{x}_M)]. \tag{43}$$

Now, we solve Eq. (40) for $\mathbf{a}(\mathbf{x})$ and we arrive at

$$\mathbf{a}(\mathbf{x}) = \mathbf{A}^{-1}(\mathbf{x})\mathbf{B}(\mathbf{x})\mathbf{U}_s. \tag{44}$$

Substituting the above relation in Eq. (36) we get

$$u_h(\mathbf{x}) = \sum_{i=1}^M \phi_i(\mathbf{x})u_i = \Phi^T(\mathbf{x})\mathbf{U}_s, \tag{45}$$

where $\Phi(\mathbf{x})$ is the vector of MLS shape functions corresponding to M nodes in the support domain of the point \mathbf{x} and we can get

$$\Phi^T(\mathbf{x}) = [\phi_1(\mathbf{x}) \ \phi_2(\mathbf{x}) \ \cdots \ \phi_M(\mathbf{x})] = \mathbf{p}^T(\mathbf{x})\mathbf{A}^{-1}(\mathbf{x})\mathbf{B}(\mathbf{x}). \tag{46}$$

The shape function $\phi_i(\mathbf{x})$ for the i th node is defined by

$$\phi_i(\mathbf{x}) = \sum_{j=1}^m p_j(\mathbf{x})(\mathbf{A}^{-1}(\mathbf{x})\mathbf{B}(\mathbf{x}))_{ji} = \mathbf{p}^T(\mathbf{x})(\mathbf{A}^{-1}\mathbf{B})_i. \tag{47}$$

We use the quartic spline function as the weight function in MLS approximation

$$W(\mathbf{x} - \mathbf{x}_i) = \begin{cases} 1 - 6r_i^2 + 8r_i^3 - 3r_i^4, & r_i \leq 1, \\ 0, & r_i > 1, \end{cases} \tag{48}$$

in which $r_i = \frac{\|\mathbf{x} - \mathbf{x}_i\|}{r_w}$, is the size of the support domain for the weight function.

5.5 Formulation of meshless methods based on local weak form

The MLPG method is constructed based on the weak form over local sub-domain such as Ω_s that is a small region considered for any point in the global domain.

We have $\Omega = \bigcup_{s=1}^n \Omega_s$ in which the local sub-domains overlap each other. The local sub-domains for any region have different geometric shapes such as circle and rectangular. In this paper we use rectangular shape for any sub-domain according to Figure 1. The local weak form of the time discrete scheme (18) is to the following form:

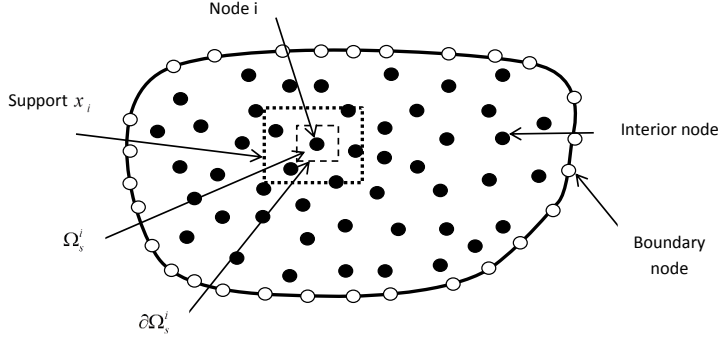


Figure 1: Local boundaries and the domain of definition of MLS approximation

$$\begin{cases} i \int_{\Omega_s^i} \Psi_1^n w d\Omega + \tau \beta \cdot \int_{\Omega_s^i} \nabla \Psi_1^n w d\Omega + \frac{\tau}{2} \int_{\Omega_s^i} \Delta \Psi_1^n w d\Omega = i \int_{\Omega_s^i} \Psi_1^{n-1} w d\Omega - \tau \varepsilon \int_{\Omega_s^i} (|\Psi_1^{n-1}|^2 + \alpha |\Psi_2^{n-1}|^2) \Psi_1^{n-1} w d\Omega, \\ i \int_{\Omega_s^i} \Psi_2^n w d\Omega + \tau \beta \cdot \int_{\Omega_s^i} \nabla \Psi_2^n w d\Omega + \frac{\tau}{2} \int_{\Omega_s^i} \Delta \Psi_2^n w d\Omega = i \int_{\Omega_s^i} \Psi_2^{n-1} w d\Omega - \tau \varepsilon \int_{\Omega_s^i} (\alpha |\Psi_1^{n-1}|^2 + |\Psi_2^{n-1}|^2) \Psi_2^{n-1} w d\Omega, \end{cases} \quad (49)$$

where w is the test function and we consider the quartic spline function (48). Using the divergence theorem we have

$$\begin{cases} i \int_{\Omega_s^i} \Psi_1^n w d\Omega + \tau \beta \cdot \int_{\Omega_s^i} \nabla \Psi_1^n w d\Omega + \frac{\tau}{2} \left(\int_{\partial \Omega_s^i} \frac{\partial \Psi_1^n}{\partial \vec{n}} w d\Gamma - \int_{\Omega_s^i} \nabla \Psi_1^n \nabla w d\Omega \right) \\ = i \int_{\Omega_s^i} \Psi_1^{n-1} w d\Omega - \tau \varepsilon \int_{\Omega_s^i} (|\Psi_1^{n-1}|^2 + \alpha |\Psi_2^{n-1}|^2) \Psi_1^{n-1} w d\Omega, \\ i \int_{\Omega_s^i} \Psi_2^n w d\Omega + \tau \beta \cdot \int_{\Omega_s^i} \nabla \Psi_2^n w d\Omega + \frac{\tau}{2} \left(\int_{\partial \Omega_s^i} \frac{\partial \Psi_2^n}{\partial \vec{n}} w d\Gamma - \int_{\Omega_s^i} \nabla \Psi_2^n \nabla w d\Omega \right) \\ = i \int_{\Omega_s^i} \Psi_2^{n-1} w d\Omega - \tau \varepsilon \int_{\Omega_s^i} (\alpha |\Psi_1^{n-1}|^2 + |\Psi_2^{n-1}|^2) \Psi_2^{n-1} w d\Omega, \end{cases} \quad (50)$$

where Ω_s^i is a rectangular domain over the point i . Now, we select M nodal points on the considered domain that some of them are on the boundary of domain. Considering the homogenous Neumann boundary conditions and substituting the approximate formula (45) or (35) into the local integral equation (50) yield

$$\left\{ \begin{aligned} & i \sum_{j=1}^M \left[\int_{\Omega_s^i} \phi_j w d\Omega + \tau \beta \cdot \int_{\Omega_s^i} \nabla \phi_j w d\Omega - \frac{\tau}{2} \int_{\Omega_s^i} \nabla \phi_j \nabla w d\Omega \right] \Psi_{1,j}^n \\ & = i \sum_{j=1}^M \left[\int_{\Omega_s^i} \phi_j w d\Omega \right] \Psi_{1,j}^{n-1} - \tau \varepsilon \sum_{j=1}^M \left[\int_{\Omega_s^i} \left(\left| \sum_{k=1}^M \phi_k \Psi_{1,k}^{n-1} \right|^2 + \alpha \left| \sum_{k=1}^M \phi_k \Psi_{2,k}^{n-1} \right|^2 \right) \phi_j w d\Omega \right] \Psi_{1,j}^{n-1}, \\ & i \sum_{j=1}^M \left[\int_{\Omega_s^i} \phi_j w d\Omega + \tau \beta \cdot \int_{\Omega_s^i} \nabla \phi_j w d\Omega - \frac{\tau}{2} \int_{\Omega_s^i} \nabla \phi_j \nabla w d\Omega \right] \Psi_{2,j}^n \\ & = i \sum_{j=1}^M \left[\int_{\Omega_s^i} \phi_j w d\Omega \right] \Psi_{2,j}^{n-1} - \tau \varepsilon \sum_{j=1}^M \left[\int_{\Omega_s^i} \left(\alpha \left| \sum_{k=1}^M \phi_k \Psi_{1,k}^{n-1} \right|^2 + \left| \sum_{k=1}^M \phi_k \Psi_{2,k}^{n-1} \right|^2 \right) \phi_j w d\Omega \right] \Psi_{2,j}^{n-1}, \end{aligned} \right. \tag{51}$$

in which $\Psi_{r,j}^n = \Psi_r(\mathbf{x}_j, t_n)$ for $r = 1, 2$ and $j = 1, 2, \dots, M$. Now, doing the numerical integrations we can obtain the following N by N system

$$\begin{bmatrix} A_1 & \\ & A_2 \end{bmatrix}_{N \times N} \begin{bmatrix} \Psi_1^n \\ \Psi_2^n \end{bmatrix}_{N \times 1} = \begin{bmatrix} B_1 & \\ & B_2 \end{bmatrix}_{N \times N} \begin{bmatrix} \Psi_1^{n-1} \\ \Psi_2^{n-1} \end{bmatrix}_{N \times 1}.$$

Note for evaluating the integrals that appear in the MLPG method, we use the 8-points Gauss integration quadrature.

6 Numerical results

In this section we present the numerical results of the proposed methods on four test problems. We test the accuracy and stability of the methods described in this paper by performing the mentioned schemes for different values of h and τ . We performed our computations using **Matlab** 7 software on a Pentium IV, 2800 MHz CPU machine with 2 Gbyte of memory. In this paper, we use the following error norms

$$\|\Psi_1^{Error}\| = \left\| \left| \Psi_1^{N_T, \frac{\tau}{2}} \right| - \left| \Psi_1^{N_T, \tau} \right| \right\|_{\infty}, \quad \|\Psi_2^{Error}\| = \left\| \left| \Psi_2^{N_T, \frac{\tau}{2}} \right| - \left| \Psi_2^{N_T, \tau} \right| \right\|_{\infty},$$

where $\Psi_j^{N_T, \tau}$ for $j = 1, 2$, are approximate solution at τ time. Also, $\|\bullet\|_\infty$ denotes the vector infinity norm.

6.1 Test Problem 1.

6.1.1 System of two nonlinear Schrödinger equations; Single soliton:

In this test problem, we solve system (9) and $\sigma_{11} = \sigma_{22} = 1$, $\sigma_{12} = \sigma_{21} = e$, where α, v and e are constants. The analytical solution to this problem with $\mu = 2$ is given by [Bhatt and Khaliq (2014)]

$$\Psi_j(x, t) = \sqrt{\frac{2\alpha}{1+e}} \operatorname{sech}(\sqrt{2\alpha}(x-vt)) e^{i\{vx - [\frac{v^2}{2} - \alpha]t\}}, \quad j = 1, 2. \tag{52}$$

Figure 2 shows graphs of $|\Psi_1| + |\Psi_2|$ at time $T = 10$ using the RBFs collocation method with $h = 1/40$, $\tau = 10^{-4}$ and $c = 0.43$ for Test problem 1. Figure 3 presents graphs of exact and approximation solutions and absolute error for $|\Psi_1|$ using the RBFs collocation method at time $T = 10$ with $h = 1/40$, $\tau = 10^{-4}$ and $c = 0.43$ for Test problem 1. Graphs of exact and approximation solutions and absolute error for $|\Psi_2|$ using the RBFs collocation method at time $T = 10$ with $h = 1/40$, $\tau = 10^{-4}$ and $c = 0.43$ for Test problem 1 are displayed in Figure 4.

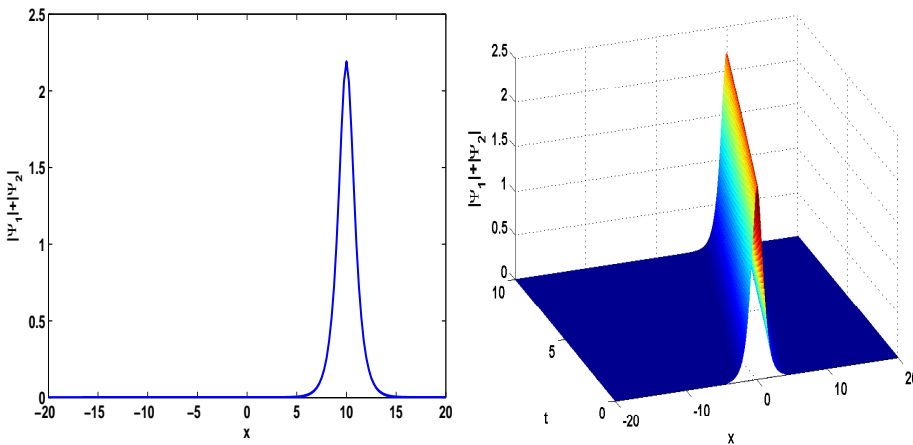


Figure 2: Graphs of single solitons at time $T = 10$ (left panel) and surface of approximation solution at different time using the RBFs collocation method with $h = 1/40$, $\tau = 10^{-4}$ and $c = 0.43$ for Test problem 1.

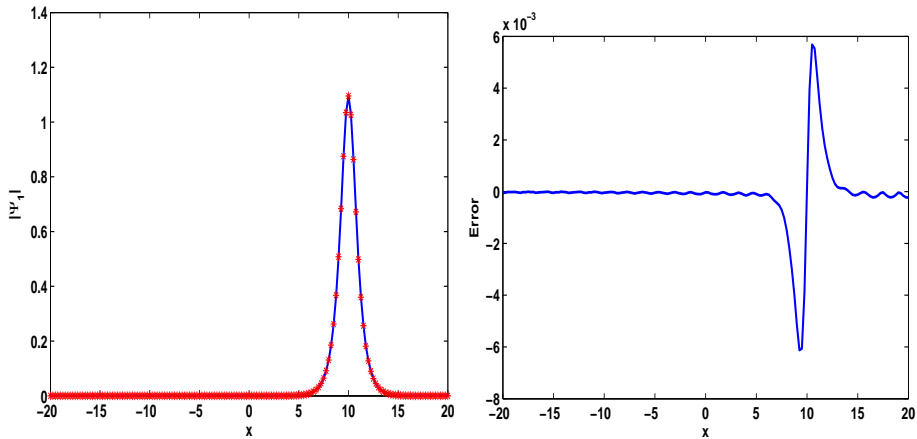


Figure 3: Graphs of exact and approximation solutions and absolute error for $|\Psi_1|$ using the RBFs collocation method at time $T = 10$ and with $h = 1/40$, $\tau = 10^{-4}$ and $c = 0.43$ for Test problem 1.

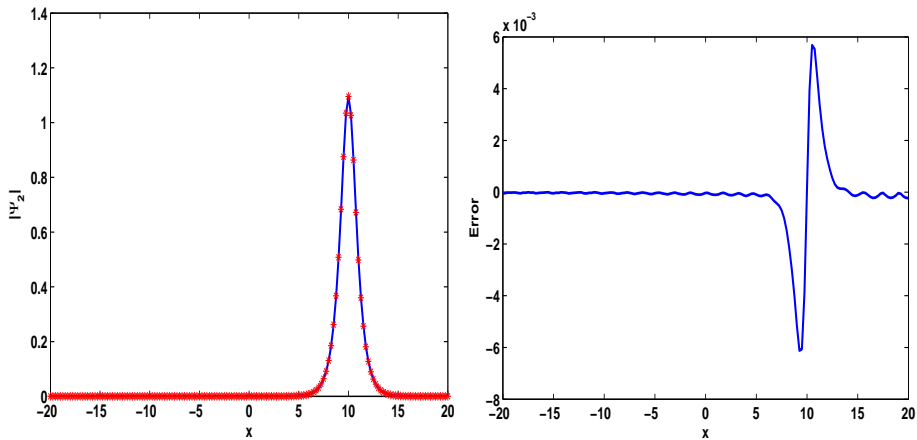


Figure 4: Graphs of exact and approximation solutions and absolute error for $|\Psi_2|$ using the RBFs collocation method at time $T = 10$ and with $h = 1/40$, $\tau = 10^{-4}$ and $c = 0.43$ for Test problem 1.

Table 1: Error obtained and conserved quantities energy and mass for single solitons for Test problem 1.

T	I_1	$\ \Psi_1\ _2$	L_∞	L_2
0	1.69704	3.6846	–	–
1	1.69707	3.6846	1.2375×10^{-4}	4.3254×10^{-3}
2	1.69711	3.6847	3.0339×10^{-4}	1.0844×10^{-3}
3	1.69712	3.6747	5.8337×10^{-4}	2.1040×10^{-3}
4	1.69720	3.6747	9.6864×10^{-4}	3.6462×10^{-3}
5	1.69724	3.6748	1.9124×10^{-3}	6.4223×10^{-3}

Table 1 presents the error obtained and conserved quantities energy and mass for single solitons for Test problem 1 with $h = 1/8$, $\tau = 1/20000$, $c = 0.43$, $v = 1$, $\mu = 2$ and $\alpha = 1$ on $\Omega = [-10, 10]$. It is clear from Table 1 that the presented method namely RBFs collocation algorithm also conserves the conserved quantities exactly, to at least five decimal places.

6.1.2 System of two nonlinear Schrödinger equations; Interaction of two solitons:

We analyze the interaction scenario of two solitons moving in opposite directions with different wave amplitudes with the RBFs collocation method. Hence, we consider system (9) with $\mu = 1$ together with initial condition [Bhatt and Khaliq (2014)]

$$\begin{cases} \Psi_1(x, 0) = \sqrt{2}r_1 \operatorname{sech}(r_1x + x_{10}) \exp(iv_1x), \\ \Psi_2(x, 0) = \sqrt{2}r_2 \operatorname{sech}(r_2x + x_{20}) \exp(iv_2x), \end{cases}$$

with $\sigma_{11} = \sigma_{22} = 1$, $\sigma_{12} = \sigma_{21} = e$, $v_1 = -v_2 = \frac{v}{4}$, $r_1 = 1.2$ and $r_2 = 1$. Now, we choose $v = 1$, $e = 1$, $\mu = 1$, $\alpha = 1$, $x_R = -x_L = 40$ and $x_{10} = -x_{20} = 20$.

Figure 5 shows graphs of two solitons interaction at different time T using the RBFs collocation method with $h = 1/2$, $\tau = 2.5^{-4}$ and $c = 0.5$ for Test problem 1. **Figure 5 presents that the two waves moving in opposite directions collide and separate after the interaction, moving forward in the same directions with the same shape and velocity, as the initial one.**

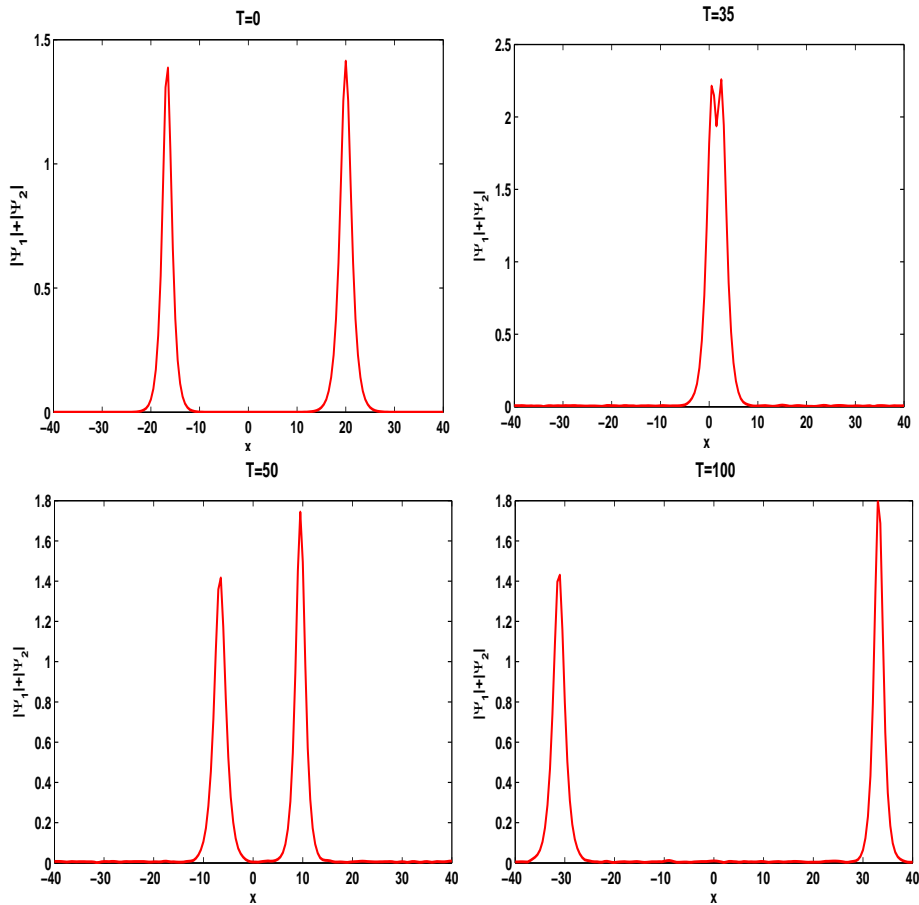


Figure 5: Graphs of two solitons interaction at different time T using the RBFs collocation method and with $h = 1/2$, $\tau = 2.5^{-4}$ and $c = 0.5$ for Test problem 1.

6.1.3 System of two nonlinear Schrödinger equations; Collision of triple solitons:

In order to show the interactions of three solitons, we solve the system (9) with the following initial conditions [Ismail (2008b)]

$$\left\{ \begin{array}{l} \Psi_1(x, 0) = \sum_{j=1}^3 \sqrt{\frac{2\alpha_j}{1+\beta}} \operatorname{sech}(\sqrt{2\alpha_j}x_j) \exp(iv_jx_j), \\ \Psi_2(x, 0) = \sum_{j=1}^3 \sqrt{\frac{2\alpha_j}{1+\beta}} \operatorname{sech}(\sqrt{2\alpha_j}x_j) \exp(iv_jx_j), \end{array} \right.$$

in which $x_1 = x$, $x_2 = x - 25$ and $x_3 = x - 50$. Also, we put $v_1 = 1$, $v_2 = 0$, $v_3 = -1$, $\alpha_1 = 1$, $\alpha_2 = 0.6$, $\alpha_3 = 0.3$, and $e = 2/3$.

Table 2: Conserved quantities energy and mass for triple solitons on interval $[-40, 40]$ for Test problem 2.

T	I_1	I_2	I_3	$\ \Psi_1\ _2$	$\ \Psi_2\ _2$	$\ \Psi_3\ _2$
0	20.0000	20.0000	20.0000	6.3443	6.3443	6.3443
1	20.0549	20.2060	20.4061	6.3660	6.3936	6.4288
2	20.0549	20.2060	20.4061	6.3660	6.3936	6.4288
3	20.0549	20.2060	20.4061	6.3660	6.3936	6.4288
4	20.0549	20.2060	20.4061	6.3660	6.3936	6.4288
5	20.0549	20.2060	20.4061	6.3660	6.3936	6.4288

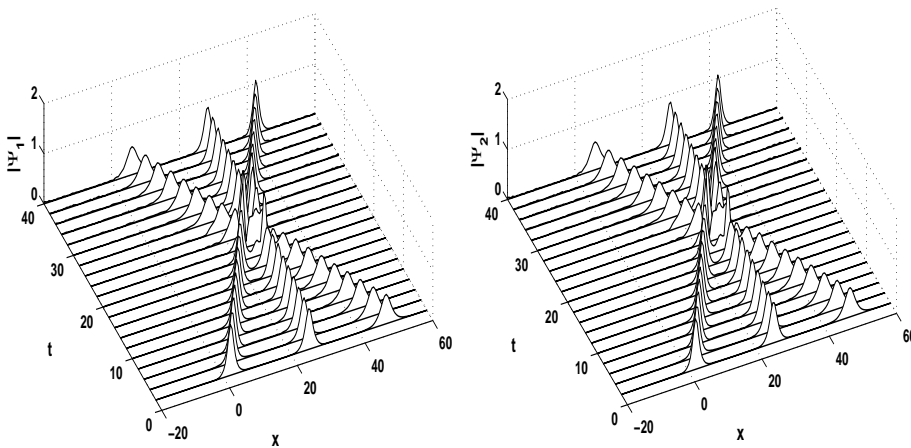


Figure 6: Graphs of three solitons interaction at different time t using the RBFs collocation method and with $h = 1/2$, $\tau = 40/40000$ and $c = 0.43$ on $[-20, 60]$ for Test problem 1.

Table 2 shows the conserved quantities energy and mass for triple solitons for Test problem 2. Figure 6 presents the graphs of three solitons interaction at different time t using the RBFs collocation method with $h = 1/2$, $\tau = 40/40000$ and $c = 0.43$ on $[-20, 60]$ for Test problem 1. Figure 6 shows the time evolution of the three-soliton interactions at different times. **Two of the three solitons are moving in**

their direction with different velocities and the third one is moving in opposite direction. It is observed that three waves interacting and leaving the interaction region unchanged in shape and velocity.

6.2 Test problem 2.

6.2.1 System of four nonlinear Schrödinger equations; Interaction of four solitons

We solve system (4) to analyze the interaction scenarios of four solitons with different wave amplitudes and different velocities. Also, we consider $\mu = 1$ with the following initial conditions [Bhatt and Khaliq (2014)]

$$\left\{ \begin{array}{l} \Psi_1(x, 0) = \sqrt{2}r_1 \operatorname{sech}(r_1x + x_{10}) \exp(iv_1x), \\ \Psi_2(x, 0) = \sqrt{2}r_2 \operatorname{sech}(r_2x - x_{10}) \exp(iv_2x), \\ \Psi_3(x, 0) = \sqrt{2}r_3 \operatorname{sech}(r_3x + x_{30}) \exp(iv_3x), \\ \Psi_4(x, 0) = \sqrt{2}r_4 \operatorname{sech}(r_4x - x_{30}) \exp(iv_4x), \end{array} \right.$$

and boundary conditions

$$\frac{\partial \Psi_j}{\partial x} = 0, \quad j = 1, 2, 3, 4, \quad x = x_L, x_R, \quad \forall t \geq 0,$$

where r_j and $v_j, j = 1, 2, 3, 4$ are arbitrary constants and $x_{10} = 10$ and $x_{30} = 30$ are initial phase constants. We select $r_1 = 1.2, r_2 = 1.2, r_3 = 1.3, r_4 = 1.4, v_1 = v_2 = \frac{v}{8}, v_3 = v_4 = \frac{v}{4}$ and $-x_L = x_R = 40$.

Table 3: Conserved quantities mass for four solitons for Test problem 2.

T	I_1	I_2	I_3	I_4
0	4.7977	4.7977	5.2015	5.6079
1	4.7980	4.7980	5.2002	5.5974
2	4.7984	4.7984	5.1969	5.5928
3	4.7987	4.7987	5.1957	5.5970
4	4.7990	4.7990	5.1988	5.6070
5	4.7994	4.7994	5.2042	5.6078

Tables 3 and 4 present the conserved quantities mass and energy, respectively, for four solitons for Test problem 2 with $h = 1/2, \tau = 25 \times 10^{-6}, c = 0.43, r_1 = 1.2,$

Table 4: Conserved quantities energy for four solitons for Test problem 2.

T	$\ \Psi_1\ _2$	$\ \Psi_2\ _2$	$\ \Psi_3\ _2$	$\ \Psi_4\ _2$
0	3.0984	3.0984	3.2249	3.3467
1	3.0984	3.0984	3.2250	3.3468
2	3.0985	3.0985	3.2250	3.3469
3	3.0985	3.0985	3.2251	3.3470
4	3.0986	3.0986	3.2252	3.3471
5	3.0986	3.0986	3.2253	3.3472

$r_2 = 1.2, r_3 = 1.3, r_4 = 1.4$. Also, we set $v = 1, e = 1, \mu = 2, \alpha = 1, v_1 = v_2 = v/8, v_3 = v_4 = v/4, x_{10} = 10, x_{30} = 30$ on $\Omega = [-40, 40]$. Similar to the previous test problems, it is clear from Tables 3 and 4 that the presented method namely RBFs collocation method also conserves the conserved quantities exactly, to at least five decimal places.

Figure 7 shows graphs of four solitons interaction at different time T using the RBFs collocation method and with $h = 1/2, \tau = 2.5^{-5}$ and $c = 0.43$ for Test problem 2.

Figure 7 shows that the amplitude of the pulses at time $T = 100$ located exactly around the amplitude of the pulses at $T = 0$, where as the amplitude of the pulses at $T = 40$ reached at the highest point. Also, in this figure, we can see that the amplitudes of the pulses are being separated [Bhatt and Khaliq (2014)].

6.3 Test problem 3.

The coupled time-dependent Schrödinger equations arise in ultrafast laser dynamics. In this test problem, we consider the initial conditions [Asadzadeh, Rostamy, and Zabihi (2013)]

$$\Psi_1(x, y, 0) = \Psi_2(x, y, 0) = \sqrt{\frac{2\alpha}{1 + \pi}} \operatorname{sech} [(x - x_{1,L})(y - y_{2,L})(x - x_{1,R})(y - y_{1,R})],$$

and boundary conditions

$$\frac{\partial \Psi_j}{\partial x} = 0, \quad j = 1, 2, \quad \forall t \geq 0,$$

where $x_{1,L} = x_{2,L} = -1$ and $y_{1,L} = y_{2,L} = -1$.

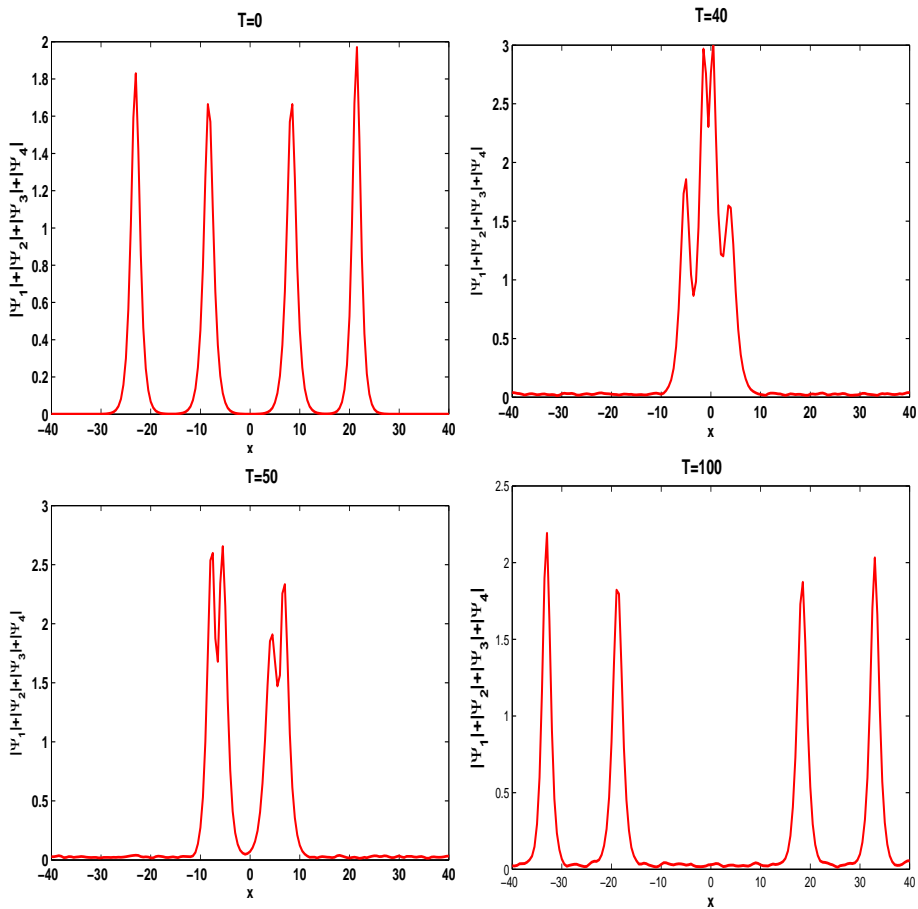


Figure 7: Graphs of four solitons interaction at different time T using the RBFs collocation method and with $h = 1/2$, $\tau = 2.5^{-5}$ and $c = 0.43$ for Test problem 2.

Since in the current example and the next test problem, there is not an exact solution, we consider the obtained solution with $h_{RS} = 2/15$ as a reference solution (as an exact solution) and then we run our MATLAB program for different values of h that results the numerical solution S_h^N (numerical solution using presented methods in the current paper). Now, interpolating the reference solution at the points with step size of h , we obtain the numerical solution S_h^I (numerical solution using

interpolating). Finally, we define the following error relation

$$E_\infty = \left\| S_h^N - S_h^I \right\|_\infty.$$

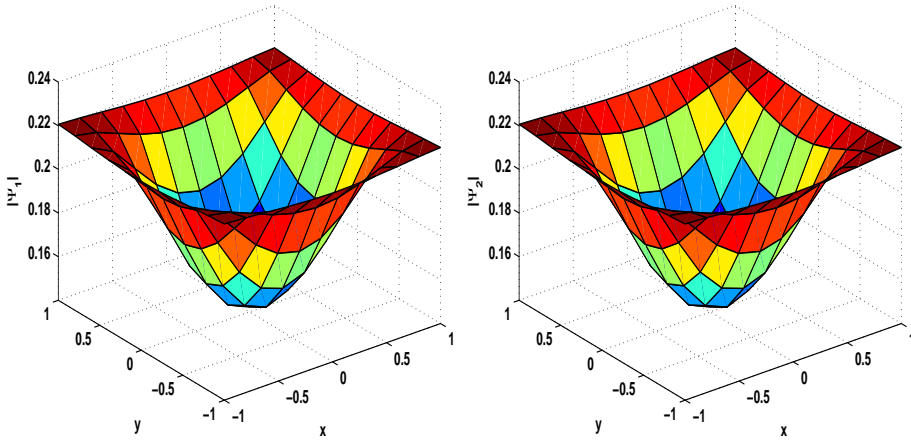


Figure 8: Graphs of approximation solution at time $T = 1$ using the RBFs meshless collocation and with $h = 1/5$, $\tau = 1/5120$, $\alpha = 0.1$, $\varepsilon = 0.9$ and $c = 0.9$ for Test problem 3.

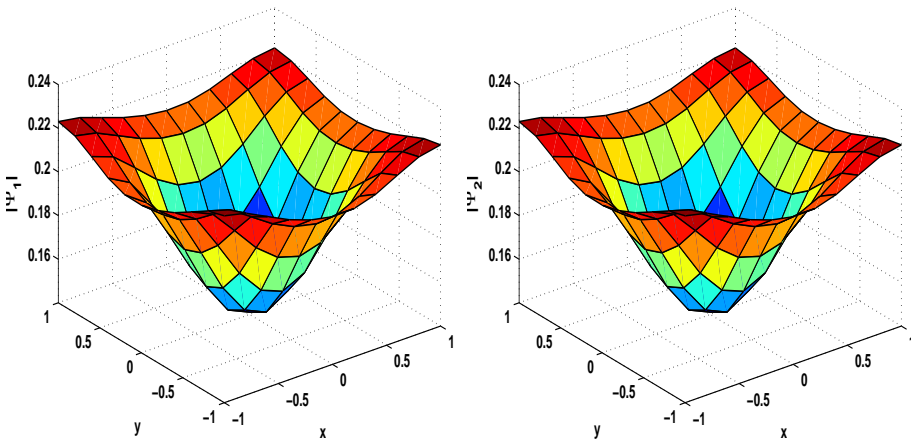


Figure 9: Graphs of approximation solution at time $T = 5$ using the RBFs meshless collocation and with $h = 1/5$, $\tau = 5/5120$, $\alpha = 0.1$, $\varepsilon = 0.9$ and $c = 0.9$ for Test problem 3.

Table 5: Errors obtained with $h = 1/5$ and $c = 0.9$ for Test problem 3 on rectangular domain $\Omega = [-1, 1] \times [-1, 1]$

τ	RBFs collocation method		MLPG method	
	$ \Psi _1^{Error}$	$ \Psi _2^{Error}$	$ \Psi _1^{Error}$	$ \Psi _2^{Error}$
1/10	—	—	—	—
1/20	2.7141×10^{-2}	2.7140×10^{-2}	3.3581×10^{-2}	3.3581×10^{-2}
1/40	2.0378×10^{-2}	2.0375×10^{-2}	2.0529×10^{-2}	2.0529×10^{-2}
1/80	1.0723×10^{-2}	1.0720×10^{-2}	1.5039×10^{-2}	1.5039×10^{-2}
1/160	7.7969×10^{-3}	7.7965×10^{-3}	1.2650×10^{-2}	1.2650×10^{-2}
1/320	4.9947×10^{-3}	4.9943×10^{-3}	8.5175×10^{-3}	8.5175×10^{-3}

Table 6: Errors obtained with $\tau = 1/80$ and $T = 1$ for Test problem 3 on rectangular domain $\Omega = [-1, 1] \times [-1, 1]$

h	RBFs method	MLPG method	LRPIM
	E_∞	E_∞	E_∞
2/4	2.3315×10^{-1}	1.1587×10^{-1}	6.2272×10^{-2}
2/8	9.0668×10^{-2}	6.6387×10^{-2}	5.8682×10^{-2}
2/10	6.0127×10^{-2}	5.4254×10^{-2}	2.6558×10^{-2}
2/14	1.0583×10^{-2}	1.7577×10^{-2}	8.6296×10^{-3}

Table 5 presents errors obtained with $h = 1/5$ and $c = 0.9$ for Test problem 3 on rectangular domain $\Omega = [-1, 1] \times [-1, 1]$. Table 5 describes that the absolute error between two successive time steps is decreasing and we can conclude that the approximate solution for the small enough time steps is tending to the exact solution. Table 6 shows errors obtained with $\tau = 1/80$ and $T = 1$ for Test problem 3. From Table 6 we can conclude that the numerical solution is convergent to the exact solution. Figure 8 shows graphs of approximation solution at time $T = 1$ using the RBFs meshless collocation technique with $h = 1/5$, $\tau = 1/5120$, $\alpha = 0.1$, $\varepsilon = 0.9$ and $c = 0.9$ for Test problem 3. Also, the graphs of approximation solution at time $T = 5$ using the RBFs meshless collocation technique with $h = 1/5$, $\tau = 5/5120$, $\alpha = 0.1$, $\varepsilon = 0.9$ and $c = 0.9$ for Test problem 3 are presented in Figure 9. Figure 10 shows the graph and contour of approximate solution using LRPIM on the domain $\Omega = [-1, 1] \times [-1, 1]$ with $h = 2/15$, $\tau = 1/80$ and final time $T = 1$ for Test problem 3. The graphs of approximation solution at time $T = 1$ using the MLPG method and with $h = 1/10$, $\tau = 1/80$, $\alpha = 0.1$ and $\varepsilon = 0.9$ for Test problem 3 are shown in Figure 11.

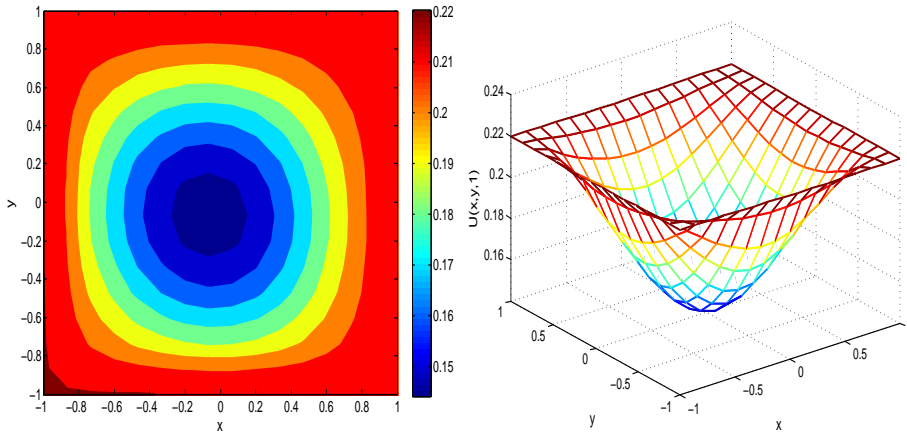


Figure 10: Graph and contour of approximate solution using LRPIM on the domain $\Omega = [-1, 1] \times [-1, 1]$ with $h = 2/15$, $\tau = 1/80$ and final time $T = 1$ for Test problem 3.

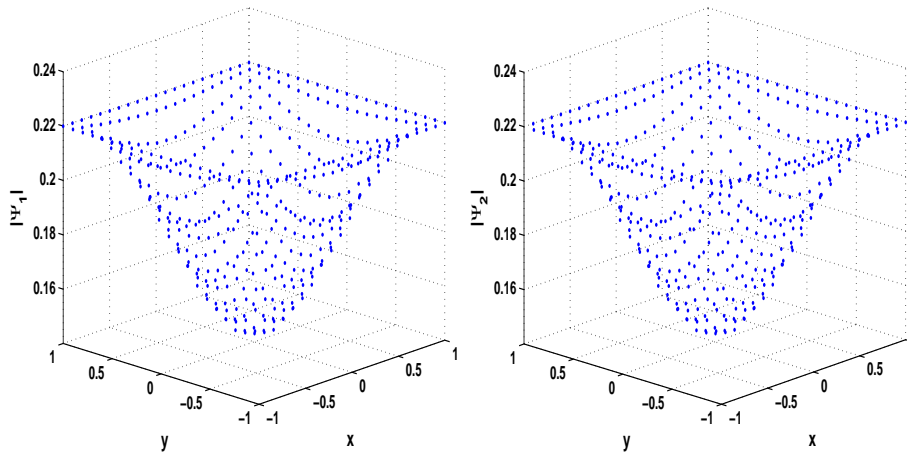


Figure 11: Graphs of approximation solution at time $T = 1$ using the MLPG method and with $h = 1/10$, $\tau = 1/80$, $\alpha = 0.1$ and $\varepsilon = 0.9$ for Test problem 3.

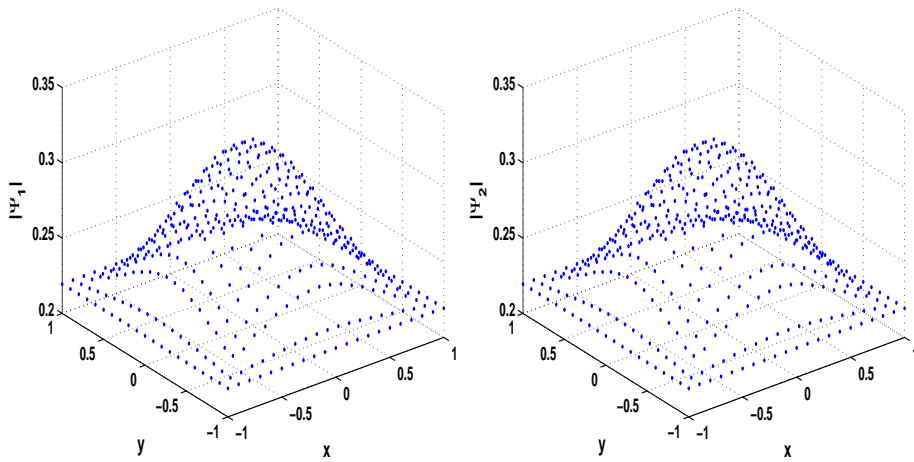


Figure 12: Graphs of approximation solution at time $T = 1$ using the MLPG method and with $h = 1/10$, $\tau = 1/80$, $\alpha = 0.1$ and $\varepsilon = 0.9$ for Test problem 4.

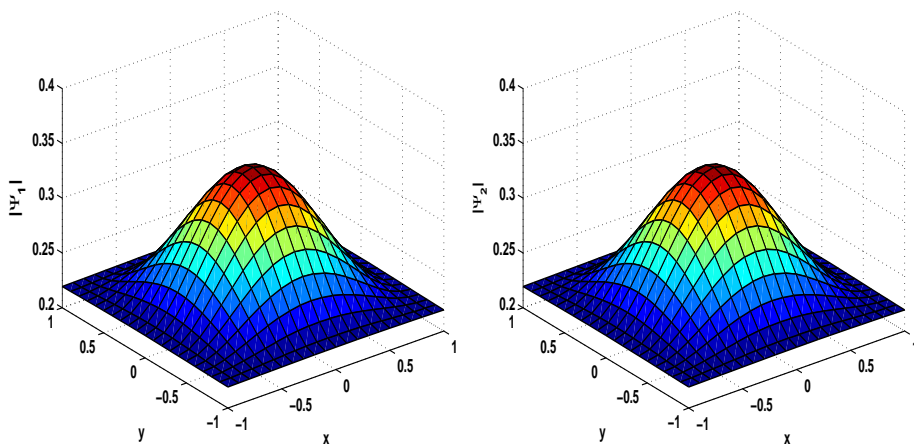


Figure 13: Graphs of approximation solution at time $T = 1$ using the RBFs meshless collocation and with $h = 1/10$, $\tau = 1/5120$, $\alpha = 0.1$, $\varepsilon = 0.9$ and $c = 0.9$ for Test problem 4.

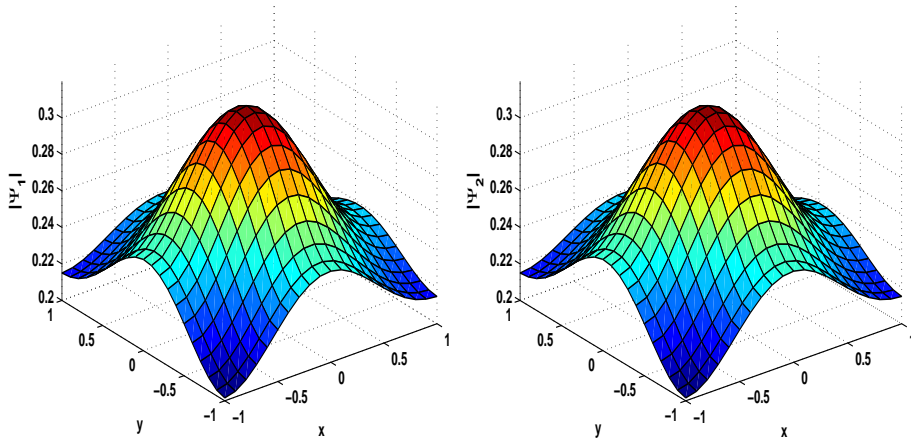


Figure 14: Graphs of approximation solution at time $T = 10$ using the RBFs meshless collocation and with $h = 1/10$, $\tau = 10/5120$, $\alpha = 0.1$, $\varepsilon = 0.9$ and $c = 0.9$ for Test problem 4.

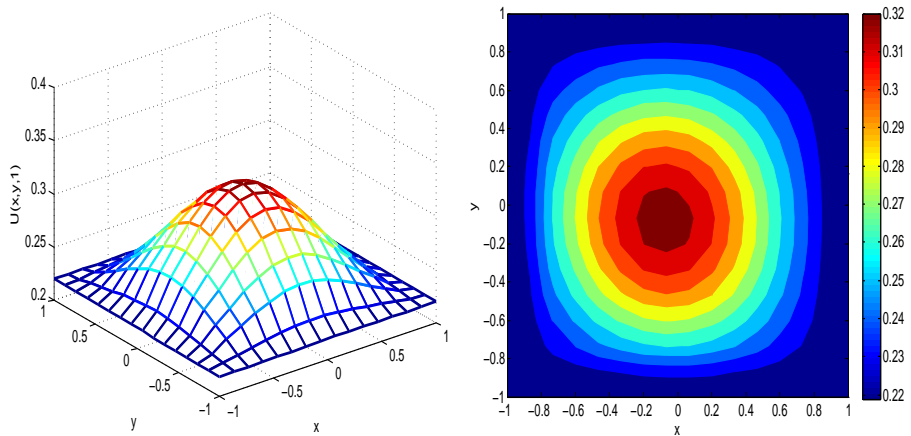


Figure 15: Graph and contour of approximate solution using LRPIM on the domain $\Omega = [-1, 1] \times [-1, 1]$ with $h = 2/15$, $\tau = 1/80$ and final time $T = 1$ for Test problem 4.

6.4 Test problem 4.

The coupled time-dependent Schrödinger equations arise in ultrafast laser dynamics. In this test problem, we consider the initial conditions [Asadzadeh, Rostamy, and Zabihi (2013)]

$$\Psi_1(x, y, 0) = \Psi_2(x, y, 0) = \sqrt{\frac{2\alpha}{1 + \pi}} \cosh[(x - x_{1,L})(y - y_{2,L})(x - x_{1,R})(y - y_{1,R})],$$

and boundary conditions

$$\frac{\partial \Psi_j}{\partial x} = 0, \quad j = 1, 2, \quad \forall t \geq 0,$$

where $x_{1,L} = x_{2,L} = -1$ and $y_{1,L} = y_{2,L} = -1$.

Table 7: Errors obtained with $h = 1/5$ and $c = 0.9$ for Test problem 4 on rectangular domain $\Omega = [-1, 1] \times [-1, 1]$

τ	RBFs collocation method		MLPG method	
	$ \Psi _1^{Error}$	$ \Psi _2^{Error}$	$ \Psi _1^{Error}$	$ \Psi _2^{Error}$
1/10	—	—	—	—
1/20	3.9664×10^{-2}	3.9670×10^{-2}	4.2158×10^{-2}	4.2158×10^{-2}
1/40	2.9384×10^{-2}	2.9389×10^{-2}	2.6541×10^{-2}	2.6541×10^{-2}
1/80	1.6694×10^{-2}	1.6650×10^{-2}	1.9677×10^{-2}	1.9677×10^{-2}
1/160	1.1548×10^{-2}	1.1548×10^{-2}	1.6548×10^{-2}	1.6548×10^{-2}
1/320	6.9938×10^{-3}	6.9940×10^{-3}	1.1061×10^{-2}	1.1061×10^{-2}

Table 8: Errors obtained with $\tau = 1/80$ and $T = 1$ for Test problem 4 on rectangular domain $\Omega = [-1, 1] \times [-1, 1]$

h	LRPIM	MLPG method	RBFs method
	E_∞	E_∞	E_∞
2/4	8.1069×10^{-2}	1.5621×10^{-1}	2.3933×10^{-1}
2/8	7.4774×10^{-2}	8.6884×10^{-2}	1.3214×10^{-1}
2/10	3.3936×10^{-2}	7.3649×10^{-2}	8.1218×10^{-2}
2/14	1.2600×10^{-2}	2.4929×10^{-2}	1.4984×10^{-2}

Table 7 presents errors obtained with $h = 1/5$ and $c = 0.9$ for Test problem 4 on rectangular domain $\Omega = [-1, 1] \times [-1, 1]$. Similar to the previous test problem, in Table 7, the absolute error between two successive time steps is decreasing and we can conclude that the approximate solution for the small enough time steps is tending to the exact solution. Table 8 demonstrates errors obtained with $\tau = 1/80$ and $T = 1$ for Test problem 4 on rectangular domain $\Omega = [-1, 1] \times [-1, 1]$. Also, Figure 12 presents the graphs of approximation solution at time $T = 1$ using the MLPG method with $h = 1/10$, $\tau = 1/80$, $\alpha = 0.1$ and $\varepsilon = 0.9$ for Test problem 4. Figure 13 shows graphs of approximation solution at time $T = 1$ using the RBFs meshless collocation with $h = 1/10$, $\tau = 1/5120$, $\alpha = 0.1$, $\varepsilon = 0.9$ and $c = 0.9$ for Test problem 4. Also, the graphs of approximation solution at time $T = 10$ using the RBFs meshless collocation method with $h = 1/5$, $\tau = 10/5120$, $\alpha = 0.1$, $\varepsilon = 0.9$ and $c = 0.9$ for Test problem 4 are presented in Figure 14. Figure 15 demonstrates the graph and contour of approximate solution using LRPIM on the domain $\Omega = [-1, 1] \times [-1, 1]$ with $h = 2/15$, $\tau = 1/80$ and final time $T = 1$ for Test problem 4.

7 Conclusion

In this paper, we solved the N -coupled nonlinear Schrödinger (CNLS) equations using the meshless method of radial basis functions and the meshless local Petrov–Galerkin (MLPG) technique and local RPIM approach. Firstly, we discretized the time derivative using the forward finite difference formula and obtained a time semi–discrete scheme. We obtained a full discrete scheme using a global form of the meshless method based on radial basis functions and Kansa’s approach. Also, using a local weak form of the meshless methods based on meshless local Petrov–Galerkin (MLPG) and LRPIM techniques, we proposed another full discretization scheme. For implementing the MLPG and LRPIM methods, firstly, we introduced the moving least squares (MLS) approximation and radial point interpolation method (RPIM) with their shape functions for approximating the solution in any subdomain. Moreover, for evaluating the integrals which appear in the MLPG and LRPIM methods, we used the 8-points Gauss quadrature rule. Since the coefficient matrices of both RBF collocation and MLPG techniques are full and ill-conditioned, we used the LU decomposition method for solving the linear system of algebraic equations which arises from the process of collocating points. The presented numerical results showed that the RBFs collocation scheme provides a simple strategy for computing long-range solitary solutions of the coupled nonlinear Schrödinger equations. Also we observed mass and energy quantities conserve exactly, to at least five decimal places. Numerical results showed the efficiency of the new three methods developed in the current paper.

References

- Abbasbandy, S.; Ghehsareh, H. R.; Alhuthali, M. S.; Alsulami, H.** (2014): Comparison of meshless local weak and strong forms based on particular solutions for a non-classical 2-D diffusion model. *Eng. Anal. Boundary Elem.*, vol. 39, pp. 121–128.
- Abbasbandy, S.; Ghehsareh, H. R.; Hashim, I.** (2013): A meshfree method for the solution of two-dimensional cubic nonlinear Schrödinger equation. *Eng. Anal. with Boundary Elem.*, vol. 37, pp. 885–898.
- Abbasbandy, S.; Shirzadi, A.** (2011): MLPG method for two-dimensional diffusion equation with Neumann's and non-classical boundary conditions. *Appl. Numer. Math.*, vol. 61, pp. 170–180.
- Ablowitz, M. J.; Clarkson, P. A.** (1991): *Solitons, Nonlinear Evolution Equations and Inverse Scattering*. Cambridge University Press, Cambridge.
- Asadzadeh, M.; Rostamy, D.; Zabihi, F.** (2013): Discontinuous Galerkin and multiscale variational schemes for a coupled damped nonlinear system of Schrödinger equations. *Numer. Methods Partial Differential Eq.*, vol. 29, pp. 1912–1945.
- Atluri, S. N.** (2004): *The Meshless Method (MLPG) for Domain and BIE Discretizations*. Tech Science Press.
- Atluri, S. N.; Shen, S.** (2002): The meshless local Petrov-Galerkin (MLPG) method: A simple and less-costly alternative to the finite element and boundary element methods. *CMES: Computer Modeling in Engineering & Sciences*, vol. 3, no. 5, pp. 11–51.
- Atluri, S. N.; Zhu, T.** (1998): A new meshless local Petrov-Galerkin (MLPG) approach in computational mechanics. *Comput. Mech.*, vol. 22, pp. 117–127.
- Bhatt, H. P.; Khaliq, A. Q. M.** (2014): Higher order exponential time differencing scheme for system of coupled nonlinear Schrödinger equations. *Appl. Math. Comput.*, vol. 228, pp. 271–291.
- Cox, S. M.; Matthews, P. C.** (2002): Exponential time differencing for stiff systems. *J. Comput. Phys.*, vol. 176, pp. 430–455.
- Dacorogna, B.** (2004): *Introduction to the Calculus of Variations*. Imperial College Press, London.
- de la Hoz, F.; Vellido, F.** (2008): An exponential time differencing method for the nonlinear Schrödinger equation. *Comput. Phys. Commun.*, vol. 179, pp. 449–456.

- Dehghan, M.; Ghesmati, A.** (2010): Numerical simulation of two-dimensional sine-Gordon solitons via a local weak meshless technique based on the radial point interpolation method (RPIM). *Comput. Phy. Commun.*, vol. 181, pp. 772–786.
- Dehghan, M.; Mirzaei, D.** (2008): The meshless local Petrov-Galerkin (MLPG) method for the generalized two-dimensional non-linear Schrödinger equation. *Eng. Anal. Bound. Elem.*, vol. 32, pp. 747–756.
- Dehghan, M.; Nikpour, A.** (2013): Numerical solution of the system of second-order boundary value problems using the local radial basis functions based differential quadrature collocation method. *Appl. Math. Model.*, vol. 37, pp. 8578–8599.
- Dehghan, M.; Salehi, R.** (2011): The solitary wave solution of the two-dimensional regularized long-wave equation in fluids and plasmas. *Comput. Phys. Commun.*, vol. 182, pp. 2540–2549.
- Dehghan, M.; Shokri, A.** (2007): A numerical method for two-dimensional Schrödinger equation using collocation and radial basis functions. *Comput. Math. Appl.*, vol. 54, pp. 136–146.
- Dehghan, M.; Taleei, A.** (2011): A Chebyshev pseudospectral multidomain method for the soliton solution of coupled nonlinear Schrödinger equations. *Comput. Phys. Commun.*, vol. 182, pp. 2519–2529.
- Dehghan, M.; Tatari, M.** (2008): Use of radial basis functions for solving the second-order equation with nonlocal boundary conditions. *Numer. Methods Partial Differential Eq.*, vol. 24, pp. 924–938.
- Fan, E. G.** (2000): Extended tanh-function method and its applications to nonlinear equations. *Phys. Let. A*, vol. 277, pp. 212–218.
- Fei, Z.; Perez-Garcia, V. M.; Vazquez, L.** (1995): Numerical simulation of nonlinear Schrödinger systems: a new conservative scheme. *Appl. Math. Comput.*, vol. 71, pp. 165–177.
- Fornberg, B.; Wright, G.; Larsson, E.** (2004): Some observations regarding interpolants in the limit of flat radial basis functions. *Comput. Math. Appl.*, vol. 47, pp. 37–55.
- Ganji, Z. Z.; Ganji, D. D.; Bararnia, H.** (2009): Approximate general and explicit solutions of nonlinear BBMB equations by Exp-Function method. *Appl. Math. Model.*, vol. 33, pp. 1836–1841.
- Gomez, C. A.; Salas, A. H.; Frias, B. A.** (2010): New periodic and soliton solutions for the generalized BBM and BBM-Burgers equations. *Appl. Math. Comput.*, vol. 217, pp. 1430–1434.

Gu, Y. T.; Zhuang, P.; Liu, F. (2010): An advanced implicit meshless approach for the non-linear anomalous subdiffusion equation. *CMES: Computer Modeling in Engineering & Sciences*, vol. 56, no. 5, pp. 303–334.

Gu, Y. T.; Zhuang, P.; Liu, Q. (2011): An advanced meshless method for time fractional diffusion equation. *International Journal of Computational Methods*, vol. 8, pp. 653–665.

Hardy, R. L. (1971): Multiquadric equations of topography and other irregular surfaces. *J. Geophys. Res.*, vol. 76, pp. 1705–1915.

Helal, M. A. (2002): Soliton solution of some nonlinear partial differential equations and its application in fluid mechanics. *Chaos Solitons Fractals*, vol. 13, pp. 1917–1929.

Helal, M. A.; Seadawy, A. R. (2009): Variational method for the derivative nonlinear Schrödinger equation with computational applications. *Physica Scripta*, vol. 80.

Helal, M. A.; Seadawy, A. R. (2011): Exact soliton solution of a D-dimensional nonlinear Schrödinger equation with damping and diffusive terms. *Zeitschrift für Angewandte Mathematik und Physik, ZAMP*, vol. 01.

Hirota, R.; Satsuma, J. (1981): Soliton solution of a coupled KdV equation. *Phys. Lett. A*, vol. 85, pp. 407–408.

Huang, C. S.; Yen, H. D.; Cheng, A. H. D. (2010): Radial basis collocation methods for elliptic boundary value problems. *Comput. Math. Appl.*, vol. 34, pp. 802–809.

Ismail, M. S. (2008): A fourth-order explicit schemes for the coupled nonlinear Schrödinger equation. *Appl. Math. Comput.*, vol. 196, pp. 273–284.

Ismail, M. S. (2008): Numerical solution of coupled nonlinear Schrödinger equation by Galerkin method. *Math. Comput. Simul.*, vol. 78, pp. 532–547.

Ismail, M. S.; Alamri, S. Z. (2004): Highly accurate finite difference method for coupled nonlinear Schrödinger equation. *Int. J. Comput. Math.*, vol. 81, pp. 333–351.

Ismail, M. S.; Taha, T. R. (2007): A linearly implicit conservative scheme for the coupled nonlinear Schrödinger equation. *Math. Comput. Simul.*, vol. 74, pp. 302–311.

Kansa, E. J. (1990): Multiquadrics A scattered data approximation scheme with applications to computational fluid dynamics - II. *Comput. Math. Appl.*, vol. 19, pp. 147–161.

- Kansa, E. J.** (1990): Multiquadrics A scattered data approximation scheme with applications to computational fluid-dynamics-I. *Comput. Math. Appl.*, vol. 19, pp. 127–145.
- Kansa, E. J.; Aldredge, R. C.; Ling, L.** (2009): Numerical simulation of two-dimensional combustion using mesh-free methods. *Eng. Anal. Bound. Elem.*, vol. 33, pp. 940–950.
- Kavitha, L.; Akila, N.; Prabhu, A.; Kuzmanovska-Barandovska, O.; Gopi, D.** (2011): Exact solitary solutions of an inhomogeneous modified nonlinear Schrödinger equation with competing nonlinearities. *Math. Comput. Model.*, vol. 53, pp. 1095–1110.
- Kazemi, B. F.; Ghoreishi, F.** (2013): Error estimate in fractional differential equations using multiquadratic radial basis functions. *J. Comput. Appl. Math.*, vol. 245, pp. 133–147.
- Kivshar, Y. S.; Agrawal, G. P.** (2003): *Optical Solutions*, Academic Press. San Diego, USA.
- Kol, G. R.; Wofo, P.** (2013): Exact solutions for a system of two coupled discrete nonlinear Schrödinger equations with a saturable nonlinearity. *Appl. Math. Comput.*, vol. 219, pp. 5956–5962.
- Kurtinaitis, A.; Ivanauska, F.** (2004): Finite difference solution methods for a system of the nonlinear Schrödinger equations. *Nonlinear Anal. Model. Control*, vol. 3, pp. 247–258.
- Liu, G. R.; Gu, Y. T.** (2005): *An Introduction to Meshfree Methods and Their Programming*. Springer Dordrecht, Berlin, Heidelberg, New York.
- Liu, Q.; Gu, Y.; Zhuang, P.; Liu, F.; Nie, Y.** (2011): An implicit RBFs meshless approach for time fractional diffusion equations. *Comput. Mech.*, vol. 48, pp. 1–12.
- Liu, S. K.; Fu, Z. T.; Liu, S. D.; Zhao, Q.** (2001): Jacobi elliptic function expansion method and periodic wave solutions of nonlinear wave equations. *Phys. Lett. A*, vol. 289, pp. 69–74.
- Matveev, V. B.; Salle, M. A.** (1991): *Darboux Transformation and Solitons*. Springer, Berlin.
- Mei, C. C.** (1989): *The Applied Dynamics of Ocean Waves*. World Scientific, Singapore.
- Mirzaei, D.; Dehghan, M.** (2010): A meshless based method for solution of integral equations. *Appl. Numer. Math.*, vol. 60, pp. 245–262.

Mirzaei, D.; Dehghan, M. (2010): Meshless local Petrov-Galerkin (MLPG) approximation to the two-dimensional sine-Gordon equation. *J. Comput. Appl. Math.*, vol. 233, pp. 2737–2754.

Miura, R. M. (1978): *Bäcklund Transformation*. Springer, Berlin.

Mohebbi, A.; Abbaszadeh, M.; Dehghan, M. (2013): The use of a meshless technique based on collocation and radial basis functions for solving the time fractional nonlinear Schrödinger equation arising in quantum mechanics. *Eng. Anal. Bound. Elem.*, vol. 37, pp. 475–485.

Mohyud-Din, S. T.; Negahdary, E.; Usman, M. (2012): A meshless numerical solution of the family of generalized fifth-order Korteweg-de Vries equations. *Int. J. Numer. Methods Heat Fluid Flow*, vol. 22, pp. 641–658.

Noor, M. A.; Noor, K. I.; Waheeda, A.; Al-Said, E. A. (2011): Some new solitary solutions of the modified Benjamin-Bona-Mahony equation. *Comput. Math. Appl.*, vol. 62, pp. 2126–2131.

Rippa, S. (1999): An algorithm for selecting a good value for the parameter c in radial basis function interpolation. *Adv. Comput. Math.*, vol. 11, pp. 193–210.

Salehi, R.; Dehghan, M. (2014): A meshless local Petrov-Galerkin method for the time-dependent Maxwell equations. *J. Comput. Appl. Math.*, vol. 268, pp. 93–110.

Sanz-Serna, J. M.; Verwer, J. G. (1986): Conservative and nonconservative schemes for the solution of the nonlinear Schrödinger equation. *IMA J. Numer. Anal.*, vol. 6, pp. 25–42.

Sheng, Q.; Khaliq, A. Q. M.; Al-Said, E. A. (2001): Solving the generalized nonlinear Schrödinger equation via quartic spline approximation. *J. Comput. Phys.*, vol. 161, pp. 400–417.

Shokri, A.; Dehghan, M. (2010): A Not-a-Knot meshless method using radial basis functions and predictor-corrector scheme to the numerical solution of improved Boussinesq equation. *Comput. Phys. Commun.*, vol. 181, pp. 1990–2000.

Shokri, A.; Dehghan, M. (2012): Meshless method using radial basis functions for the numerical solution of two-dimensional complex Ginzburg-Landau equation. *CMES: Computer Modeling in Engineering & Sciences*, vol. 34, pp. 333–358.

Sladek, J.; Sladek, V.; Hon, Y. C. (2006): Inverse heat conduction problems by meshless local Petrov-Galerkin method. *Eng. Anal. Bound. Elem.*, vol. 36, pp. 650–661.

- Sladek, J.; Sladek, V.; Krivacek, J.; Wen, P. H.; Zhang, C.** (2007): Meshless local Petrov–Galerkin (MLPG) method for Reissner–Mindlin plates under dynamic load. *Comput. Methods Appl. Mech. Engrg.*, vol. 196, pp. 2681–2691.
- Sladek, J.; Sladek, V.; Zhang, C.; Schanz, M.** (2006): Meshless local Petrov–Galerkin method for continuously nonhomogeneous linear viscoelastic solids. *Comput. Mech.*, vol. 37, pp. 279–289.
- Sladek, J.; Stanak, P.; Han, Z. D.; Sladek, V.; Atluri, S. N.** (2013): Applications of the MLPG Method in Engineering & Sciences: A Review. *CMES: Computer Modeling in Engineering & Sciences*, vol. 92, no. 5, pp. 423–475.
- Sun, J. Q.; Gu, X. Y.; Ma, Z. Q.** (2004): Numerical study of the solitons waves of the coupled nonlinear Schrödinger system. *Physica D*, vol. 196, pp. 311–328.
- Tatari, M.; Dehghan, M.** (2010): A method for solving partial differential equations via radial basis functions: Application to the heat equation. *Eng. Anal. Bound. Elem.*, vol. 34, pp. 206–212.
- Vanani, S. K.; Aminataei, A.** (2008): On the numerical solution of neural delay differential equations using multiquadric approximation scheme. *Bull. Korean Math. Soc.*, vol. 45, pp. 663–670.
- Wang, M. L.; Li, X. Z.** (2005): Applications of F-expansion to periodic wave solutions for a new Hamiltonian amplitude equation. *Chaos Solitons Fract.*, vol. 24, pp. 1257–1268.
- Wang, M. L.; Zhou, Y. B.; Li, Z. B.** (1996): Applications of a homogeneous balance method to exact solutions of nonlinear equations in mathematical physics. *Phys. Lett. A*, vol. 216, pp. 67–75.
- Wazwaz, A. M.** (2006): Exact solutions for the fourth order nonlinear Schrödinger equations with cubic and power law nonlinearities. *Math. Comput. Model.*, vol. 43, pp. 802–808.
- Wazwaz, A. M.** (2008): A study on linear and nonlinear Schrödinger equations by the variational iteration method. *Chaos, Solitons and Fractals*, vol. 37, pp. 1136–1142.
- Wazwaz, A. M.** (2009): *Partial Differential Equations and Solitary Waves Theory*. Springer, New York.
- Weiss, J.; Tabor, M.; Carnevale, G.** (1983): The Painlevé property for partial differential equations. *J. Math. Phys.*, vol. 24, pp. 522–526.
- Wendland, H.** (2005): *Scattered Data Approximation*. Cambridge Monograph on Applied and Computational Mathematics, Cambridge University Press.

Yoon, J. (1999): Spectral approximation orders of radial basis function interpolation on the Sobolev space. *SIAM J. Math. Anal.*, vol. 33, pp. 946–958.

Yoon, J. (2003): L_p -error estimates for shifted surface spline interpolation on Sobolev space. *Math. Comp.*, vol. 72, pp. 1349–1367.

Zhang, H. Q.; Meng, X. H.; Xu, T.; Li, L. L.; Tian, B. (2007): Interactions of bright solitons for the (2+1)-dimensional coupled nonlinear Schrödinger equations from optical fibres with symbolic computation. *Phys. Scr.*, vol. 75, pp. 537–542.

Zhuang, P.; Liu, F.; Anh, V.; Turner, I. (2008): New solution and analytical techniques of the implicit numerical methods for the anomalous sub-diffusion equation. *SIAM J. Numer. Anal.*, vol. 46, pp. 1079–1095.